JARO 17: 173–194 (2016)
DOI: 10.1007/s10162-016-0558-8

JARO
Journal of the Association for Research in Otolaryngology

Research Article

QTL Mapping of Endocochlear Potential Differences between C57BL/6J and BALB/cJ mice

Kevin K. Ohlemiller,[1] Anna L. Kiener,[2] and Patricia M. Gagnon[1]

[1]*Department of Otolaryngology, Central Institute for the Deaf at Washington University School of Medicine, Fay and Carl Simons Center for Hearing and Deafness, Washington University School of Medicine, 660 S. Euclid, St. Louis, MO 63110, USA*

[2]*Department of Speech and Hearing Science, Ohio State University, Columbus, OH, USA*

Received: 16 February 2015; Accepted: 25 February 2016; Online publication: 15 March 2016

ABSTRACT

We reported earlier that the endocochlear potential (EP) differs between C57BL/6J (B6) and BALB/cJ (BALB) mice, being lower in BALBs by about 10 mV (Ohlemiller et al. Hear Res 220: 10–26, 2006). This difference corresponds to strain differences with respect to the density of marginal cells in cochlear stria vascularis. After about 1 year of age, BALB mice also tend toward EP reduction that correlates with further marginal cell loss. We therefore suggested that early *sub-clinical* features of the BALB stria vascularis may predispose these mice to a condition modeling Schuknecht's strial presbycusis. We further reported (Ohlemiller et al. J Assoc Res Otolaryngol 12: 45–58, 2011) that the acute effects of a 2-h 110 dB SPL noise exposure differ between B6 and BALB mice, such that the EP remains unchanged in B6 mice, but is reduced by 40–50 mV in BALBs. In about 25 % of BALBs, the EP does not completely recover, so that permanent EP reduction may contribute to noise-induced permanent threshold shifts in BALBs. To identify genes and alleles that may promote *natural EP variation* as well as noise-related EP reduction in BALB mice, we have mapped related quantitative trait loci (QTLs) using 12 recombinant inbred (RI) strains formed from B6 and BALB (CxB1–CxB12). EP and strial marginal cell density were measured in B6 mice, BALB mice, their F1 hybrids, and RI mice without noise exposure, and 1–3 h after broadband noise (4–45 kHz, 110 dB SPL, 2 h). For unexposed mice, the strain distribution patterns for EP and marginal cell density were used to generate preliminary QTL maps for both EP and marginal cell density. Six QTL regions were at least statistically suggestive, including a significant QTL for marginal cell density on chromosome 12 that overlapped a weak QTL for EP variation. This region, termed *Maced* (Marginal cell density QTL) supports the notion of marginal cell density as a genetically influenced contributor to natural EP variation. Candidate genes for *Maced* notably include *Foxg1, Foxa1, Akap6, Nkx2-1,* and *Pax9*. Noise exposure produced significant EP reductions in two RI strains as well as significant EP increases in two RI strains. QTL mapping of the EP in noise-exposed RI mice yielded four suggestive regions. Two of these overlapped with QTL regions we previously identified for noise-related EP reduction in CBA/J mice (Ohlemiller et al. Hear Res 260: 47–53, 2010) on chromosomes 5 and 18 (*Nirep*). The present map may narrow the *Nirep* interval to a ~10-Mb region of proximal Chr. 18 that includes *Zeb1*, *Arhgap12*, *Mpp7*, and *Gjd4*. This study marks the first exploration of natural gene variants that modulate the EP. Their orthologs may underlie some human hearing loss that originates in the lateral wall.

Electronic supplementary material The online version of this article (doi:10.1007/s10162-016-0558-8) contains supplementary material, which is available to authorized users.

Correspondence to: Kevin K. Ohlemiller · Department of Otolaryngology, Central Institute for the Deaf at Washington University School of Medicine, Fay and Carl Simons Center for Hearing and Deafness · Washington University School of Medicine · 660 S. Euclid, St. Louis, MO 63110, USA. Telephone: 314 747 7179; email: kohlemiller@wustl.edu

Keywords: stria vascularis, noise-induced hearing loss, recombinant inbred, genetics, cochlea, lateral wall

INTRODUCTION

The endocochlear potential (EP) is a large positive extracellular potential (+80–110 mV, depending on species) making up part of the electrochemical gradient that drives cochlear hair cell receptor potentials (Wangemann 2006; Nin et al. 2008; Ohlemiller 2009; Hibino et al. 2010). Both single unit thresholds and compound action potential (CAP) thresholds depend on the EP, such that every millivolt of EP decline causes ~0.5–1.0 dB of threshold elevation (Sewell 1984; Ohlemiller 2009). Thus, pathology of cochlear stria vascularis, which generates the EP, would contribute to hearing loss. Schuknecht (Schuknecht et al. 1974; Schuknecht and Gacek 1993) theorized a form of presbycusis caused entirely by strial dysfunction. From his observations of temporal bones, he proposed that the initial pathology involves loss or dysfunction of strial marginal cells. While EP generation also critically involves strial intermediate and basal cells, marginal cells perform the most metabolically demanding work, potentially placing these cells uniquely at risk for pathology (Spicer and Schulte 2005).

The EP has been recorded only anecdotally in humans (Tran Ba Huy et al. 1989; Kobayashi et al. 1996), so that nearly all we can infer about strial dysfunction in human hearing derives from work in animal models, wherein both aging and noise exposure have been shown to cause EP reduction. Animal models of strial presbycusis include Mongolian gerbils, in which primary pathology of strial marginal cells may account for changes in the appearance of the stria, EP decline, and most of the observed hearing loss (Schmiedt 1993). Mouse inbred lines have been identified in which the EP remains constant over a typical lifespan (C57BL/6J [B6] and CBA/J), and in which the EP declines over the lifespan (Ohlemiller 2009). The latter include inbred BALB/cJ and CBA/CaJ mice, two popular models for hearing research (Willott et al. 1998; Ohlemiller et al. 2010b), as well as albino congenics to B6 (Ohlemiller et al. 2009). In each of these three models, the EP is essentially normal in young animals, but begins to decline after about 1 year of age. All three mouse models recapitulate the causative pattern suggested for humans, namely that the initial pathology manifests in marginal cells. The most prominent principle that derives from the finding of two *kinds* of mouse inbred lines (i.e., those with and without EP decline) is that there must be a genetic component to age-associated EP decline, although environmental and/or stochastic factors appear involved, and any *pro-strial presbycusis genes* likely work permissively with other factors (Ohlemiller 2009).

BALB mice stand out among animal models of strial presbycusis in potentially informative ways. First, the typical EP in young BALB mice falls within normal limits for mice, yet compared to young B6 mice it is significantly lower by about 10 mV (Ohlemiller et al. 2006). This difference may account for the fact that young BALB mice have ~10 dB higher ABR and CAP thresholds than B6 mice (Ohlemiller 2002). One may question, therefore, whether young BALBs should ever qualify as having a normal EP. However, if we could measure the EP in a large group of people who do not meet clinical criteria for hearing loss we would likely encounter EP variation exceeding 10 mV. Second, the young BALB stria possesses fewer, larger marginal cells than the young B6 stria, and significant further losses with age occur only in BALBs (Ohlemiller et al. 2006). Thus marginal cell density can account for the lifelong pattern of EP divergence between BALB and B6 mice, perhaps by altering the stoichiometry of critical strial ion pumps, channels, and exchangers (Diaz et al. 2007). The apparent strial origin of EP decline in BALBs means that it is not necessary to invoke any particular state of the organ of Corti: Given that both BALB and B6 mice exhibit severe hair cell loss by 1 year of age (Willott et al. 1998), EP decline in only BALBs contradicts any claim that hair cell loss prevents otherwise inevitable and universal EP decline by reducing the current load on the stria.

Effects of noise exposure on stria vascularis have long been known from animal studies (e.g., Duvall et al. 1974; Ulehlova 1983). However, relatively few have included EP measurement (e.g., Vassout 1984; Ikeda et al. 1988; Ahmad et al. 2003), and parametric studies have been performed only in guinea pigs (Konishi et al. 1979; Salt and Konishi 1979; Ide and Morimitsu 1990; Wang et al. 1992) and mice (Wang et al. 2002; Hirose and Liberman 2003). In guinea pigs, the EP may temporarily rise or fall after noise, depending apparently on noise parameters. In mice, only EP reduction has been reported, the extent of which depends on noise level, and on genetic background. We showed that for a single intense exposure (4–45 kHz, 110 dB SPL, 2 h) B6 mice show no EP reduction, while CBA/J, CBA/CaJ, and BALB mice exhibit acute EP losses of 40–50 mV (Ohlemiller and Gagnon 2007; Ohlemiller et al. 2011). Moreover, while to our knowledge, all studies of the EP following noise indicate eventual full recovery, about 25 % of BALB mice showed incomplete recovery, so that permanent EP reduction may contribute to some noise-induced permanent threshold shifts (NIPTS).

Mapping studies of acute EP reduction in CBA/J mice yielded weak QTLs on chromosomes 5 and 16, and a significant QTL (*Nirep*) on proximal chromosome 18 (Ohlemiller et al. 2010a). Different inheritance patterns of the EP-reduction phenotype in CBA/J and BALB mice suggested that at least some non-overlapping loci or alleles are involved.

From the preceding, BALB mice emerge as a particularly intriguing genetic model of strial presbycusis, and both acute and permanent EP reduction by noise. Young unexposed BALBs have a minimal *clinical* phenotype, yet by virtue of starting life with too few marginal cells, they may be predisposed toward EP decline over their lifespan. In addition, as the only animal model presently identified that is prone to permanent noise-related EP decline, they may harbor alleles with similar-acting human orthologs. To map predisposing genes for late-onset EP reduction in BALBs would be prohibitively difficult, as it would require phenotyping based on EP reduction that would only appear in some old mice. However, if the EP and anatomic differences between *young* BALB and B6 mice hold the keys to later age-related changes, we may be able to map related QTLs for both EP and marginal cell density using young animals. Here, we describe preliminary mapping of EP variance in young unexposed and acute, noise-exposed BALB mice using 12 recombinant inbred (RI) strains formed from inbred B6 and BALB lines (CxB1–CxB12).

METHODS

Animals

Procedures were approved by the Washington University Institutional Animal Care and Use Committee. Physiologic recording, morphometry, and mapping were conducted using C57BL/6J (B6, $n=25$), BALB/cJ (BALB, $n=34$), reciprocal F1 hybrids (that is, separate lines by parent gender) ($n=29$), and CxB RI series mice (see Table 1), all derived from breeders purchased from The Jackson Laboratory (JAX). Mice were 2–5 months of age at the time of evaluation. All samples were randomly composed by gender, and no gender effects were detected in any feature reported here.

The CxB RI series includes a total of 13 strains, termed CxB1 to CxB13 (Table 1). These lines were generated from C57BL/6ByJ and BALBc/ByJ, thus the CxB series does not provide an exact genetic match to C57BL/6J and BALB/cJ mice used in our original experiments. Table 1 includes coat color for each RI strain, since this may reflect strial pigmentation and thereby impact the stress- or aging-resistance of the stria (Conlee et al. 1986, 1988; Ohlemiller et al. 2009). No clear pattern by coat color (e.g., agouti, albino) emerged in the data we report. We were not able to include CxB13 mice in our study, as these mice invariably had bullas filled with dense infectious material, sometimes combined with an abnormally shaped bulla. This feature was unique to CxB13 mice so that it either reflects new mutations within this line, or these mice may segregate multiple alleles from both strains that jointly promote this phenotype. This feature may be of interest for genetic middle ear pathology, but was not useful for the present work. Also, CxB8 mice were highly prone to sometimes lethal audiogenic seizures, which could be prevented by slowly ramping up exposure levels over 1–2 min.

TABLE 1
Full names, EP sample sizes, and coat colors of CxB RI strains

Strain name	*Number examined*		*Coat color*
	No noise	*Noise*	
CXB1/ByJ	14	11	Agouti
CXB2/ByJ	11	10	Agouti
CXB3/ByJ	10	6	Albino
CXB4/ByJ	14	8	Chocolate brown
CXB5/ByJ	14	12	Albino
CXB6/ByJ	12	7	Chocolate brown
CXB7/ByJ	15	11	Black
CXB8/HiAJ	10	9	Black
CXB9/HiAJ	10	8	Agouti
CXB10/HiAJ	11	11	Albino
CXB11/HiAJ	13	14	Brown agouti
CXB12/HiAJ	13	10	Albino

CAP and EP recording

For each animal, CAP and EP recordings were conducted in the same terminal procedure, so that each animal was assessed once, immediately prior to sacrifice. Acute post-noise EP and CAP measures were obtained 1–3 h after exposure. Sample sizes for EP recordings are shown in Table 1. CAP recordings were conducted in a subset of animals encompassing 6–20 unexposed mice and 4–15 noise-exposed mice of each strain. Animals were anesthetized (60 mg/kg sodium pentobarbital, IP) and positioned ventrally in a custom headholder. Core temperature was maintained at 37.5 ± 1.0 °C using a thermostatically controlled heating pad in conjunction with a rectal probe (Yellow Springs Instruments Model 73A). An incision was made along the midline of the neck and soft tissues were blunt dissected and displaced laterally to expose the trachea and animal's left bulla. A tracheostomy was then made and the musculature over the bulla was cut posteriorly to expose the bone overlying the round window. Using a hand drill, a small hole was made over the round window. The recording electrode was a modified platinum needle electrode (Grass) insulated

with epoxy except for the tip, which was inserted into round window antrum using a micromanipulator. Additional platinum electrodes inserted into the neck musculature and hind leg served as reference and ground, respectively. Electrodes were led to a Grass P15 differential amplifier (100–3000 Hz, ×100), then to a custom amplifier providing another ×1000 gain, then digitized at 30 kHz using a Cambridge Electronic Design Micro1401 in conjunction with SIGNAL™ and custom signal averaging software operating on a 120 MHz Pentium PC. Sine wave stimuli generated by a Hewlett Packard 3325A oscillator were shaped by a custom electronic switch to 5 ms total duration, including 1 ms rise/fall times. The stimulus was amplified by a Crown D150A power amplifier and output to a KSN1020A piezo ceramic speaker located 7 cm directly lateral to the left ear. Stimuli were presented free field and calibrated using a B&K 4135 ¼ inch microphone placed where the external auditory meatus would normally be. Toneburst stimuli at each frequency and level were presented 100 times at 3/s. The minimum sound pressure level required for visual detection of a response (N_1) was determined at 2.5, 5, 10, 20, 28.3, and 40 kHz, using a 5 dB minimum step size.

For EP recordings a hole was made in the left cochlear capsule directly over scala media of the lower basal turn, using a fine drill. Glass capillary pipettes (40–80 MΩ) filled with 0.15 M KCl were mounted on a hydraulic microdrive (Frederick Haer) and advanced until a stable positive potential was observed that did not change with increased electrode depth. The signal from the recording electrode was led to an AM Systems Model 1600 intracellular amplifier. A silver/silver chloride ball inserted into the neck muscles served as ground. Statistical evaluations included comparison of EP by condition within strain (noise/no noise) by *t* tests (Fig. 7), and linear correlation of EP on marginal cell density (Fig. 3) (Sigmastat). Correlations were tested both for scatter plots for individual animals of all strains, and for mean EP versus mean marginal cell density by strain.

Noise exposure

Noise exposures were performed in a foam-lined, single-walled soundproof room (IAC). The noise exposure apparatus consisted of a 21 × 21 × 11 cm wire cage mounted on a pedestal inserted into a B&K 3921 turntable. To ensure a uniform sound field, the cage was rotated at 1 revolution/80 s within a 42 × 42-cm metal frame. A Motorola KSN1020A piezo ceramic speaker (four total) was attached to each side of the frame. Opposing speakers were oriented non-concentrically, parallel to the cage, and driven by separate channels of a Crown D150A power amplifier. Broadband noise was generated by General Radio 1310 generators and band-passed at 4–45 kHz by Krohn-Hite 3550 filters. Noise levels at various points in the exposure cage, measured using a B&K 4135 ¼ inch microphone in combination with a B&K 2231 sound level meter, ranged from 110–113 dB SPL. Mice were exposed in pairs for 2.0 h.

Tissue processing, sectioning, and marginal cell counts

Based on previous evidence that the EP in mice correlates with strial marginal cell density (Ohlemiller et al. 2006, 2009, 2010b), some cochleas used for EP/CAP recordings were evaluated morphometrically. Only unexposed animals were examined (see Fig. 3 for sample sizes.). Immediately after recording, animals were overdosed and perfused transcardially with cold 2.0 % paraformaldehyde/2.0 % glutaraldehyde in 0.1 M phosphate buffer (pH 7.4). Each cochlea was rapidly isolated, immersed in the same fixative, and the stapes was immediately removed. Complete infiltration of the cochlea by fixative was ensured by making a small hole at the apex of the cochlear capsule, and gently circulating the fixative over the cochlea using a transfer pipet. After decalcification in 0.1 M sodium EDTA for 72 h, cochleas were post-fixed in buffered 1 % osmium tetroxide, dehydrated in an ascending acetone series, and embedded in Epon. Left cochleas were sectioned in the mid-modiolar plane at 4.0 µm, then stained with toluidine blue for bright field viewing with a Nikon Optiphot™ light microscope using a ×100 oil objective and a calibrated grid ocular. Typically 50 sections were obtained from each cochlea, spanning 200 µm centered on the modiolar *core*.

For each animal, 10 mid-modiolar sections distributed evenly over the 200-µm-sectioned distance were analyzed by an observer blinded to strain. Following our previous studies, measures were obtained for the upper basal turn. Marginal cell nuclei were counted in an 80 µm linear segment of stria centered at the midpoint. Counts for each animal were averaged across sections to yield a mean for that animal then a grand average was obtained for each strain.

QTL mapping

RI strains are generated through serial inbreeding of hybrid offspring from two highly polymorphic inbred lines. For each strain of an RI series, serial inbreeding establishes homozygosity at nearly all loci for the allele of just one of the parent strains. This process will be random, except that the total number of recombinations will be limited by the size of the RI series, and each strain may inherit large regions in which no recombination has occurred. For every strain in a commercial RI series, the strain distribution pattern of a dense microsatellite marker set has been established, so that the contribution of one parent

strain versus the other is known for closely spaced intervals throughout the genome. This permits preliminary mapping of any phenotype through comparison of the strain distribution pattern of the phenotype of interest with that of the marker set. This can be carried out using online utilities such as WebQTL (www.GeneNetwork.org). RI series formed from different parent strains have been used to map QTLs for a host of phenotypes, including hearing loss (Hitzemann et al. 2001; Noben-Trauth et al. 2010; Nagtegaal et al. 2012). The single major requirement is that the parent strains must differ with regard to the phenotype of interest. Thus, having found that the typical EP differs between B6 and BALB mice, we were constrained to use an RI series constructed from these lines. The CxB series is the oldest and smallest commercial RI series. This potentially limits the resolution of mapping due to fewer recombinations across the series, and also increases the chance that some QTLs will reflect fortuitous co-alignment of unrelated alleles and traits that just happen to have the same strain distribution pattern. As a result, some QTLs may represent false positives.

Mapping was accomplished using the online WebQTL mapping utility at GeneNetwork (www.GeneNetwork.org) by simply entering mean or categorical EP values by strain. Genome-wide significance levels were determined by permutation testing (1000 permutations). Maps generated by WebQTL feature two statistical thresholds for evaluation of QTLs (see Figs. 4, 5, and 8). Significant linkage indicates a p value of 0.05, while suggestive linkage indicates a p value that yields, on average, one false positive per whole genome scan. This is a very permissive threshold, but it is useful because it calls attention to loci that merit follow-up. WebQTL also permits the optional use of parental strain phenotypes in map generation. Maps generated using parental data are equivalent to substituting a one-tailed t test for a two-tailed t test, effectively halving stringency requirements for linkage. This is appropriate when one strain dominates the F1 phenotype, as is the case here, since B6 alleles appear dominant over BALB alleles in both exposed and unexposed F1s (Ohlemiller et al. 2011). Omitting parental data, however, can usefully unmask surprising contributions of recessive alleles in both strains. Strain contributions revealed by inclusion or exclusion of parental data are expressed as additive values. In this case additive values indicate that extent to which alleles from either parent strain increase the EP in unexposed or exposed mice. To gain the advantages of both approaches, we compared maps generated with, and without, parental data (see Figs. 4, 5 and 8). Additive values are presented graphically in Figures. 4, 5, and 8, and numerically in Tables S1 and S2.

Normal EP mapping in unexposed mice

EPs in unexposed mice were relatively narrowly distributed across strains. Nevertheless, when recording the EP it is far more likely to obtain artifactually low values than high values, simply because of the invasiveness of the procedure. Since the accuracy of any map can only be as good as the EP data, we were faced with the issue of how best to characterize the EP by strain. We applied three schemes based on the assumption that our *lowest* values were most likely to be in error. These schemes respectively included all the data, dropped the lowest value, or dropped the two lowest values for each strain (see Figs. 2 and 4).

Mapping of acute noise-related EP changes

As we show, noise exposure significantly acutely reduced the EP in some strains and increased the EP in others. Since the initial EP also differed by strain, neither final EP, nor mean EP change (noise versus no noise) appeared a completely satisfactory way to characterize the data. WebQTL alternately allows the use numerically defined categories for mapping. In addition to mean EP change, we tested two categorical schemes. The first utilized simple categories, whereby a significant EP reduction was scored −1, no change was scored 0, and a significant increase was scored +1. The second scheme (not shown) attempted to enhance sensitivity to allele combinations by scoring a large mean EP reduction (BALB, CxB4) as −2 and a smaller mean EP reduction (CxB5) as −1. These two schemes yielded similar results. We also considered the possibility that apparent EP increases in two strains (CxB3, CxB8) were statistical flukes, and in one categorical scheme scored these as 0's. When parental data were omitted, the resulting map was flat, virtually devoid of any visually discernible QTL peaks (not shown). In part because the maps we show reproduce some earlier results (Ohlemiller et al. 2010a), we interpret this as evidence that the acute EP increases we show are real and genetically based.

Once QTL regions were identified, we sought candidate genes through a combination of cochlear-relatedness and polymorphic character between C57BL/6J and BALB/cJ. To establish cochlear-relatedness, genes lying within 10 % of peak log-odds (LOD) scores were queried using the MGI Database with keywords inner ear, cochlea, deafness, lateral wall, spiral ligament, stria vascularis, and potassium. Some QTL regions were quite narrow, and keyword searches returned few or no genes. In such cases, all polymorphic genes were included. Single nucleotide polymorphisms (SNPs) that were consid-

TABLE 2

Relevant genes within suggestive QTL regions for normal (non-noise-exposed) mice

Based on MGI, OVID/Medine, Google scholar searches on keywords cochlea, inner ear, lateral wall, stria vascularis, spiral ligament

C = Nonsynonymous Coding
US = Upstream
5' = 5'UTR; 3' = 3'UTR

Chr.	QTL	**Which Alleles Increase the EP	***Gene	***Product	#Peak LOD for Closest Marker	*B6 versus BALB Polymorphisms	Key Reference
10	1	B6	**Atoh7**	Atonal homolog 7	2.9	C	Ikeda et al., 2014
10			**Sirt1**	Surtuin 1	2.9	C	Takumida et al., 2014
10	2	B6	**Grip1**	Glutamate receptor-interacting protein 1	2.5	C, 5', 3', US	Dong et al., 1999
10			**Lrig3**	Leucine-rich repeats and IgG-like domains 3	2.5	C, 5', 3', US	Abraira et al., 2010
10			**Mbd6**	Methyl-CpG binding domain protein 6	2.5	C	Jung et al., 2013
10			**Chop/Gadd153**	C/EBP homologous protein 10	2.5	US	Fujinami et al., 2012
10			**Arhgap9**	Rho GTPase activating protein 9	2.5	C, 5'	Furukawa et al., 2001
10			**Gli1**	GLI family zinc finger 1	2.5	C	Braunstein et al., 2009
10			**Lrp1**	Low density lipoprotein receptor-related protein 1	2.5	C, 5', US	Adams, J.C., 2009
10			**Stat6**	Signal transducer and activator of transcription 6	2.5	C, 5', 3', US	Kim et al., 2011
10			**Nab2**	NGFI-A binding protein 2	2.5	C, 3'	O'Donovan et al., 1999
10			**Mip/Aqp0**	Aquaporin 0	2.5	US	Han et al.,. 2005
10			**Stat2**	Signal transducer and activator of transcription 2	2.5	C, 5', 3', US	Kim et al., 2011
10			**Neurod4**	Neurogenic differentiation 4	2.5	3'	Bell et al., 2008
12	*Maced*	B6	**Foxg1**	Forkhead box G1	3.3	C, US	Pauley et al., 2006
12			**Arhgap5/Gap5**	Rho GTPase activating protein 5	2.3	C, US	Howard, 2012
12			**Akap6**	A kinase (PRKA) anchor protein 6	2.3	C, US	Diviani et al., 2013
12			**Eapp**	E2F-associated phosphoprotein	2.3	C, 3'	Walters et al., 2014
12			**Nkx2-1/Titf1**	NK2 homeobox 1	3.0	3'	Varma et al., 2012
12			**Pax9**	Paired box 9	4.5	US	Chatterjee et al., 2010
12			**Slc25a21**	Solute carrier (mitochondrial oxodicarboxylate)	4.1	US	Santagati et al., 2003
12			**Mipol1**	Mirror-image polydactyly gene 1 homolog	4.1	C, 5', 3'	Malik, 2014
12			**Foxa1/Tcf3a**	Forkhead box A1	4.1	C	Cirillo and Zaret, 2007
12			**Sstr1**	Somatostatin receptor 1	4.1	3'	Bodmer et al., 2012
12			**Clec14a**	C-type lectin domain family 14a	4.1	C, 5', 3'	Wragg et al., 2014
13	4	BALB	**Cd180/Ly78**	Cd180 antigen	2.6	C, 3'	Chaplin et al., 2009
13			**Mast4**	Microtubule associated serine/threonine kinase 4	2.6	C, 3', US	Garland et al., 2008
15	5	BALB	**Asap1**	ArfGAP with ankyrin repeat and PH domain 1	3.1	C, 3'	Jamesdaniel et al., 2009
15			**Oc90/PLA2L**	Otoconin 90	3.1	C, US	Yang et al., 2011
15			**Kcnq3**	K+ voltage-gated channel, subfamily Q, member 3	3.1	US	Holt and Corey, 1999
15			**Lrrc6**	Leucine rich repeat containing 6	3.1	C, 3'	Wansleeben and Meijlink, 2011
15			**Tg**	Thyroglobulin	3.1	C, 3', US	Royaux et al., 2000
15	6	BALB	**Cacng2**	Ca++ channel, voltage-dependent, gamma 2	1.5	5', 3', US	Yoshimura et al., 2014
15			**Mfng**	O-fucosylpeptide 3-B-N-acetylglucosaminyltransferase	1.5	5', US	Kiernan, 2013
15			**Triobp**	TRIO and F-actin binding protein	1.5	C, 5', US	Shahin et al., 2006
15			**Sox10**	Sex determining region Y-box 10	1.5	3', US	Watanabe et al., 2000
15			**Pla2g6**	Phospholipase A2, group VI	1.5	C	Alagramam et al., 2014
15			**Maff**	Musculoaponeurotic fibrosarcoma oncogene, protein F	1.5	5', 3', US	Jamesdaniel et al., 2009
15			**Kcnj4**	K+ inwardly-rectifying channel, subfamily J, member 4	1.5	3', US	Alsaber et al., 2006
15			**Pdgfb**	Platelet derived growth factor, B polypeptide	1.5	C, 5', 3', US	Bonkowski et al., 2011
15			**Atf4/CREB2**	Activating transcription factor 4	1.5	5', US	Fujinami et al., 2010
15			**Arhgap8**	Rho GTPase activating protein 8	1.5	C, 5', US	Scheffer et al., 2007
15			**Ppara/Nr1c1**	Peroxisome proliferator activated receptor alpha	2.1	3', US	Marzolo and Farfán, 2011
15			**Pkdrej**	Polycystic kidney disease (polycystin) and REJ	2.1	C, 3', US	Asai et al., 2010
15			**Celsr1**	Cadherin, EGF LAG seven-pass G-type receptor 1	2.1	C, 5', US	Curtin et al., 2003
15			**Rabl2**	RAB, member RAS oncogene family-like 2	3.1	C, 5', 3', US	Pereira-Leal and Seabra, 2000

*SNP Browser (GeneNetwork.org)
**WebQTL (GeneNetwork.org)
***MGI Database
#From Table S1
Chr. 12 based on Figure 5.

ered included upstream, nonsynonymous coding, intronic with start gained, 5′ UTR, and 3′ UTR. Polymorphisms were identified using the SNP browser feature of GeneNetwork. Our primary goal was to be inclusive, so that supplementary tables S1 and S2 cover a large number of genes in all clearly visually discernible peaks from any mapping scheme. Our results, however, focus on polymorphic genes within suggestive or significant QTLs that gained additional relevance from OVID/Medline and Google Scholar searches (Tables 2 and 3). QTL regions on chromosomes 5 and 18 that emerged from the BALB data overlap with regions previously identified in CBA/J mice (Ohlemiller et al. 2010a). For that reason, we also consider BALB versus CBA/J polymorphisms in those regions (Table 3).

RESULTS

Strain distribution of CAP thresholds, EPs, and marginal cell density in unexposed mice

CAP thresholds in unexposed mice were generally similar across strains (Fig. 1). All showed some degree of threshold elevation at higher frequencies. This is in keeping with the fact that both B6 and BALB harbor alleles at multiple loci that promote progressive threshold elevation (Erway et al. 1993; Nemoto et al. 2004), in addition to the *Cdh23*^{753A} allele (Johnson et al. 2000; Noben-Trauth et al. 2003). No correlation was found between CAP thresholds and baseline EP across strains (not shown), owing presumably to the independence of early hair cell pathology and factors that set the EP.

TABLE 3

Relevant genes within suggestive QTL regions for noise-related EP change

Based on MGI, OVID/Medine, Google scholar searches on keywords cochlea, inner ear, lateral wall, stria vascularis, spiral ligament

C = Nonsynonymous Coding
US = Upstream
5' = 5'UTR; 3' = 3'UTR
ND = No Differences

Chr.	QTL	**Which Alleles Increase the EP	***Gene	***Product	#Peak LOD for Closest Marker	Polymorphisms *BALB vs. B6	*BALB vs. CBA/J	Key Reference
5	7	B6	**Akap9/Yotiao**	Protein kinase A anchor protein 9	1.8	C	C, US, 5'	Summers et al., 2010
5			**Fzd1**	Frizzled homolog 1	1.8	3', 5', US	3', 5'	Bohnenpoll et al., 2014
5			**Cdk14/Pftk1**	Cyclin-dependent kinase 14	1.8	C, 5', 3', US	3'	Kaldis and Pagano, 2009
5			**Shh**	Sonic hedgehog	1.5	C, US	ND	Riccomagno et al., 2002
5			**Emilin1**	Elastin microfibril interfacer 1	1.5	C, US, 3'	ND	Dakshnamurthy et al., 2012
5			**Mpv17**	Mitochondrial inner membrane protein	1.3	US	ND	Meyer zum Gottesberge et al., 2012
5			**Hmx1**	H6 homeobox 1	1.3	US	ND	Wang and Lufkin, 2005
5			**Wfs1**	Wolfram syndrome 1 homolog	1.4	3', US	ND	Cryns et al., 2003
5			**Otop1**	Otopetrin	1.5	C, US	ND	Hughes et al., 2006
5			**Wdr1**	WD repeat domain 1	1.5	3', US	ND	Oh et al., 2002
9	8	BALB	**Ncam1**	Neural cell adhesion molecule 1	1.7	3', US		Cai et al., 2012
9			**Hspb2**	Heat shock protein 2	1.7	C		Leonova et al., 2002
9			**Cryab**	Crystallin, alpha B	1.7	5', US		Gratton et al., 2011
9			**Pou2af1**	POU domain, class 2, associating factor 1	1.7	US		Yoon et al., 2011
9			**Rdx**	Radixin	1.7	3'		Kitajiri et al., 2004
9			**Elmod1**	ELMO/CED-12 domain containing 1	1.7	3'		Johnson et al., 2012
9			**Cyp19a1**	Cytochrome P450, family 19a, peptide 1	1.7	3'		Meltser et al., 2008
9	9	BALB	**Tmie**	Transmembrane inner ear	1.6	US		Mitchem et al., 2002
18	*Nirep*	B6	**Crem**	cAMP responsive element modulator	2.3	US	ND	Harris et al., 2008
18	↓		**Zeb1**	Zinc finger E-box binding homeobox 1	2.3	C, 3'	C	Hertzano et al., 2011
18			**Arhgap12**	Rho GTPase activating protein 12	2.3	US, 3'	ND	Rudnicki et al., 2014
18			**Kif5b**	Kinesin family member 5B	2.3	C, 3', US	C, US	Horn et al., 2013
18			**Mkx**	Mohawk homeobox	2.3	5', 3'	3'	Liu et al., 2010
18			**Armc4**	Armadillo repeat containing 4	2.3	3'	ND	Hjeij et al., 2013
18			**Mpp7**	MAGUK p55 subfamily member 7	2.3	3', US	ND	Xiao et al., 2012
18			**Wac**	WW domain adaptor w/coiled-coil	2.3	C, 5', 3', US	C, 5', US	Joachim et al., 2012
18			**Gjd4**	Gap junction protein, delta 4	2.3	5'(start gain), 3'	ND	Oyamada et al., 2013
18			**Greb1l**	Growth regulation by estrogen	2.3	3'	ND	Plouhinec et al., 2014
18			**Gata6**	GATA binding protein 6	1.8	US, 5', 3'	ND	Ronaghi et al., 2014

*SNP Browser (GeneNetwork.org)
**WebQTL (GeneNetwork.org)
***MGI Database
#From Table S2

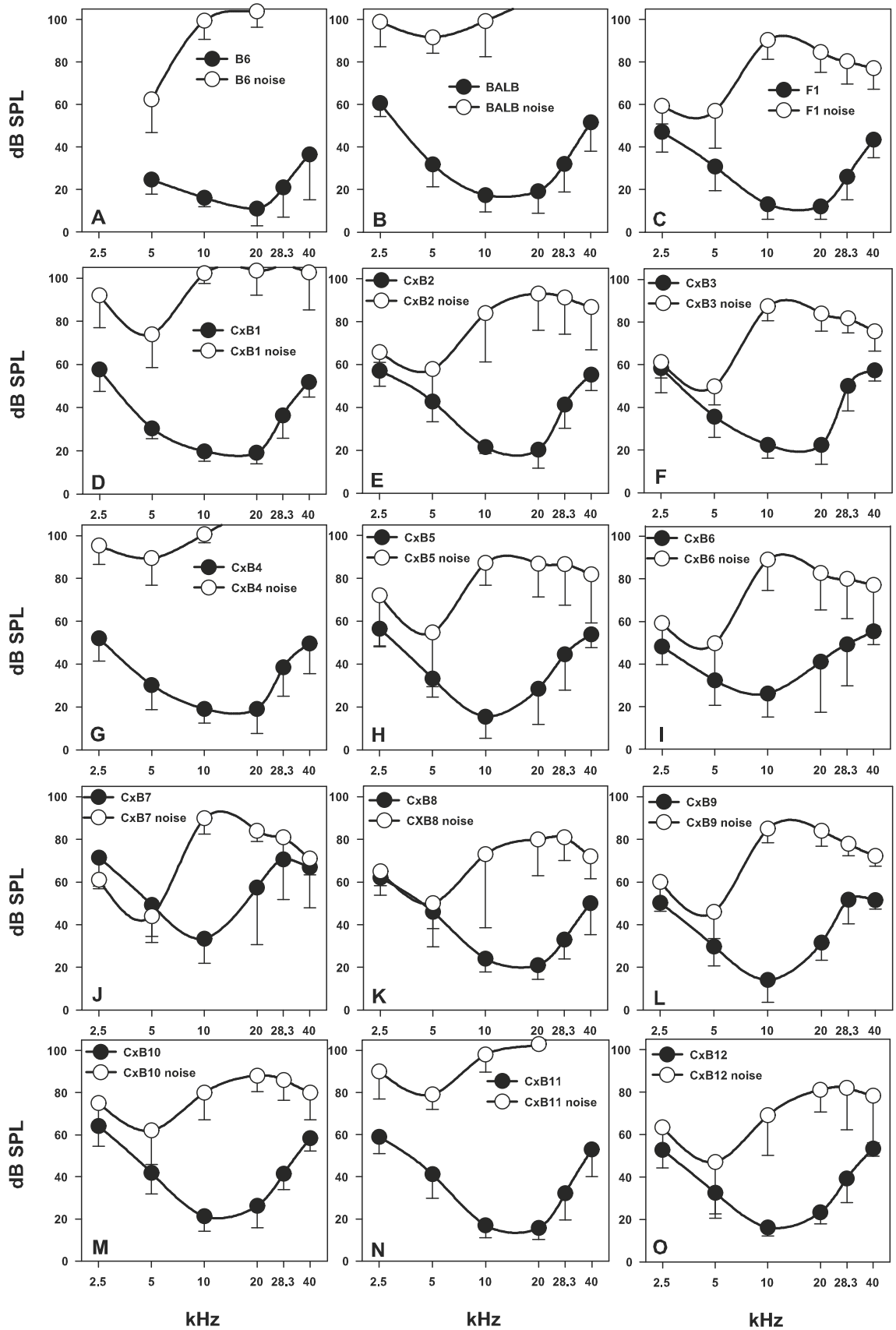
dB SPL
kHz
A
B6
B6 noise
B
BALB
BALB noise
C
F1
F1 noise
D
CxB1
CxB1 noise
E
CxB2
CxB2 noise
F
CxB3
CxB3 noise
G
CxB4
CxB4 noise
H
CxB5
CxB5 noise
I
CxB6
CxB6 noise
J
CxB7
CxB7 noise
K
CxB8
CXB8 noise
L
CxB9
CxB9 noise
M
CxB10
CxB10 noise
N
CxB11
CxB11 noise
O
CxB12
CxB12 noise
0
20
40
60
80
100
2.5
5
10
20
28.3
40

FIG. 1. (**A–O**) Mean (−standard deviation) left ear CAP thresholds by mouse strain and condition (unexposed, noise-exposed). Data for B6 mice (**A**) were obtained before low-frequency measures had been extended to 2.5 kHz. Post-noise thresholds were obtained in the acute period after exposure, immediately before EP measures. Off-scale data at higher frequencies (**A**, **B**, **D**, **G**) reflect cases where most animals gave no response at the limits of the speaker.

EP distributions for the parental strains, reciprocal F1 hybrids, and RI strains are ordered by mean in Figure 2. Two of the three highest mean EPs were found in the hybrids, indicating that one or both parent strains harbor incompletely- or non-penetrant alleles favoring higher EPs than appear in either parent strain. The overall range of mean EPs was fairly narrow at ~11 mV. Across all groups, EP data were narrowly distributed, with nearly all values lying between 90–120 mV. Ordering of strains by mean EP revealed a gradual progression lacking clear discontinuities, consistent with a contribution to phenotype of multiple alleles. The BALB parent strain showed the lowest EPs, suggesting that none of the RI strains segregate all the alleles that tend to depress the EP in BALB mice.

No significant correlation was found between marginal cell density in the cochlear upper base and the EP. This was the case for both group mean data (Fig. 3) and individual animal data (not shown). Of the data in Figure 3, three of the five data points corresponding to EPs >110 mV and marginal cell densities >6.3 cells/80 μm were associated with the B6 parent strain and the two F1 hybrid lines. Thus, in B6 × BALB crosses, higher marginal cell density, like a higher EP, appears dominant.

QTLs for EP and marginal cell density

As stated in "Methods", mapping strategies differed either with respect to the number of lowest EP data points dropped for each group (0, 1, or 2), or with respect to the use of parental data in map generation. Resulting maps (Fig. 4) indicated many of the same QTL regions. A single strategy was tested for mapping

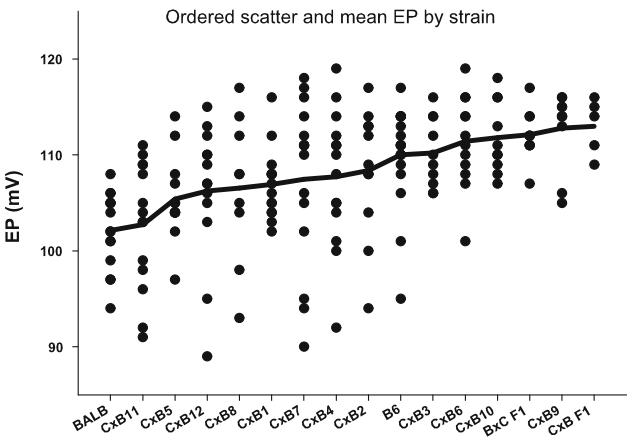

FIG. 2. Scatter plot of EP values for unexposed B6, BALB, F1 hybrids, and all RI strains examined, ranked by mean EP.

of marginal cell density (mean data without parents) (Fig. 5). All maps featured a number of non-significant peaks, some of which are likely to be false positives. Across all mapping conditions, only QTL regions on chromosomes 10, 12, 13, and 15 were at least suggestive. QTLs on chromosomes 13 and 15 appear to hold BALB alleles that tend to increase the EP (see additive effects in Table S1). Table S1 lists relevant genes in many visually discernible peaks in Figures 4 and 5, while Table 2 and subsequent text focus on polymorphic genes within suggestive or significant QTL regions. As we consider in the "Discussion", genes expressed in either the lateral wall or organ of Corti could influence the EP. We therefore include genes predominantly expressed in either location.

Chromosome 10

Chromosome 10 holds two suggestive QTLs. Centrally there is a region spanning with ~3 Mb with a peak LOD score of 2.9. This small region holds few polymorphic genes. Two relevant genes that differ with respect to coding are *Atoh7* (Atonal homolog 7) and *Sirt1*, the latter a protective protein strongly expressed in stria and spiral ligament (Takumida et al. 2014). The second QTL lies distally and spans ~10 Mb with a peak LOD score of 2.5. There are several potentially relevant genes in the interval. Glutamate receptor-interacting protein 1 (*Grip1*) is the most highly polymorphic known gene within the QTL span, although it has no published cochlear function (Dong et al. 1999). *Lrig3*, *Gli1*, and *Neurod4* are involved in inner ear development (Bell et al. 2008; Braunstein et al. 2009; Abraira et al. 2010). C/EBP homologous protein 10 (*Ddit3/CHOP*) is expressed in the metabolically stressed stria and spiral ligament (Fujinami et al. 2012). Its primary function is not known, but it may promote oxidative stress. *Arhgap9* encodes a Rho-GTPase involved in cytoskeletal remodeling (Furukawa et al. 2001), although its cochlear role is not well defined. *Lrp1* encodes a receptor for connective growth factor, and is expressed in type I and IV fibrocytes, stria, and spiral limbus (Adams 2009). *Stat6* and *Stat2* mediate cochlear inflammatory responses (Kim et al. 2011). *Aqp0* is one of several aquaporins expressed in the ear (Han et al. 2005).

Chromosome 12

We have repeatedly observed a correlation between EP and strial marginal cell density in mice, although no relation emerged across the CxB RI series (Fig. 3). We nevertheless tested whether EP and marginal cell density yield similar QTL maps. Mapping of mean

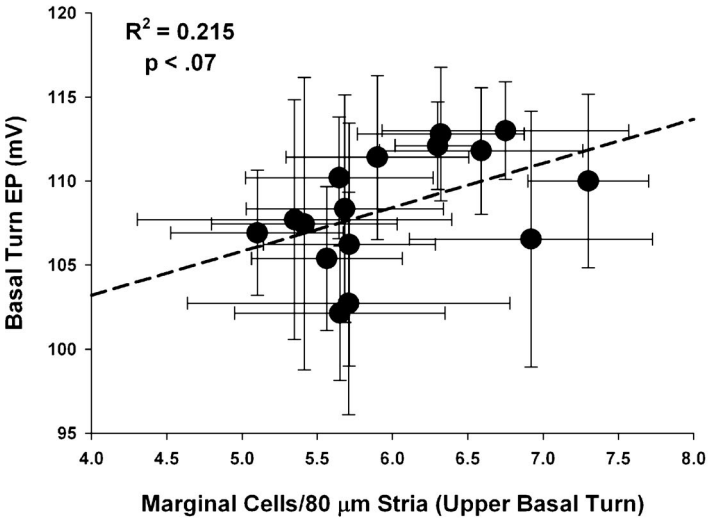

	Marg. Cell Ears	EP Ears
CxB F1	2	10
BxC F1	4	5
B6	4	18
BALB	8	15
CxB1	8	14
CxB2	6	11
CxB3	5	10
CxB4	5	14
CxB5	6	13
CxB6	6	12
CxB7	7	15
CxB8	5	9
CxB9	5	10
CxB10	6	10
CxB11	5	14
CxB12	7	13

FIG. 3. Correlation of mean EP and mean marginal cell density across strains was not significant. Error bars in *X* and *Y* are standard deviations. Sample sizes for deriving means are given in the table at right.

marginal cell density by strain yielded a significant QTL on mid-chromosome 12 (Fig. 5). A suggestive LOD score was reached for a segment spanning the ~47–72 Mb region, while significance (LOD 4.5) was reached for a very narrow segment (<1 Mb) near 58 Mb. We have termed this region *Maced* (Marginal cell density QTL). The *Maced* interval showed general overlap with a weak QTL for EP (~48-58 Mb, Figs. 4 and 5). The overlapping QTLs suggest that one or more genes in this region may partly modulate the EP in young mice through an influence on marginal cell density. Additive scores for QTLs related to both marginal cell density and EP were negative (Fig. 3), indicating that B6-derived alleles increase both marginal cell density and EP, consistent with the phenotype of the parent strains. Mapping using parental data, which would be expected to amplify the influence of B6 alleles, increased the LOD score for this region to 5.2, while retaining the same interval (not shown). In assessing genes on chromosome 12, LOD scores for both EP and marginal cell density were considered jointly, so that the metric associated with the higher LOD score appears in Table S1 and forms the basis for consideration of candidate genes (Table 2). Polymorphic genes within the suggestive QTL interval include forkhead box transcription factors *Foxg1* and *Foxa1*, which have been tied to inner ear development (Pauley et al. 2006; Cirillo and Zaret 2007). The product of NK-2 homeobox 1 (*Nkx2-1*) interacts developmentally with grainyhead-like 2 (*Grhl2*), which is deafness gene *DFNA28* (Varma et al. 2012). *Arhgap5* encodes another Rho-GTPase, albeit it with no clear cochlear role (Howard 2012). *Akap6* may modulate the conductance of KCNE1/KCNQ1, which jointly gate K^+ entry into scala media from strial marginal cells (Kang et al. 2008; Diviani et al. 2013). The only known gene lying within the significant QTL interval (LOD 4.5) is *Pax9*, a gene likely involved in inner ear development, but whose specific role is not clear (Chatterjee et al. 2010). *Pax9* polymorphisms between B6 and BALB include at least 16 upstream and intronic differences (Tables S1 and 2), but it is not clear that these impact function.

Chromosome 13

On Chromosome 13, BALB alleles act to increase the EP. This chromosome holds a very narrow suggestive QTL spanning less than 0.5 Mb. The only known polymorphic genes within this interval are *Cd180* and *Mast4*, for which no tie to lateral wall development or function was found (Garland et al. 2008; Chaplin et al. 2009).

Chromosome 15

BALB alleles on chromosome 15 also act to increase the EP. The distal half of this chromosome holds two narrow suggestive QTLs, an ~18 Mb span (from ~59–77-Mb) and a ~13-Mb

FIG. 4. QTL maps for mean EP generated using WebQTL. Plots are taken directly from the GeneNetwork website. Four mapping strategies were compared, depending upon whether parent strain data were used, and whether raw EP data were used (**A, B**), or the lowest 1 or 2 EP values were dropped from each group prior to mapping (**C, D**). Some of the same QTL regions recurred in multiple maps, although LOD scores depended on mapping strategy. *Blue traces* indicate LOD scores by chromosome (left *Y* axis), while *red* and *green traces* (additive effects, right *Y* axis) respectively indicate regions where B6 or BALB alleles tended to increase the EP (see Tables S1 and 2). Significance of LOD scores (*horizontal lines*, see text) was determined by WebQTL.

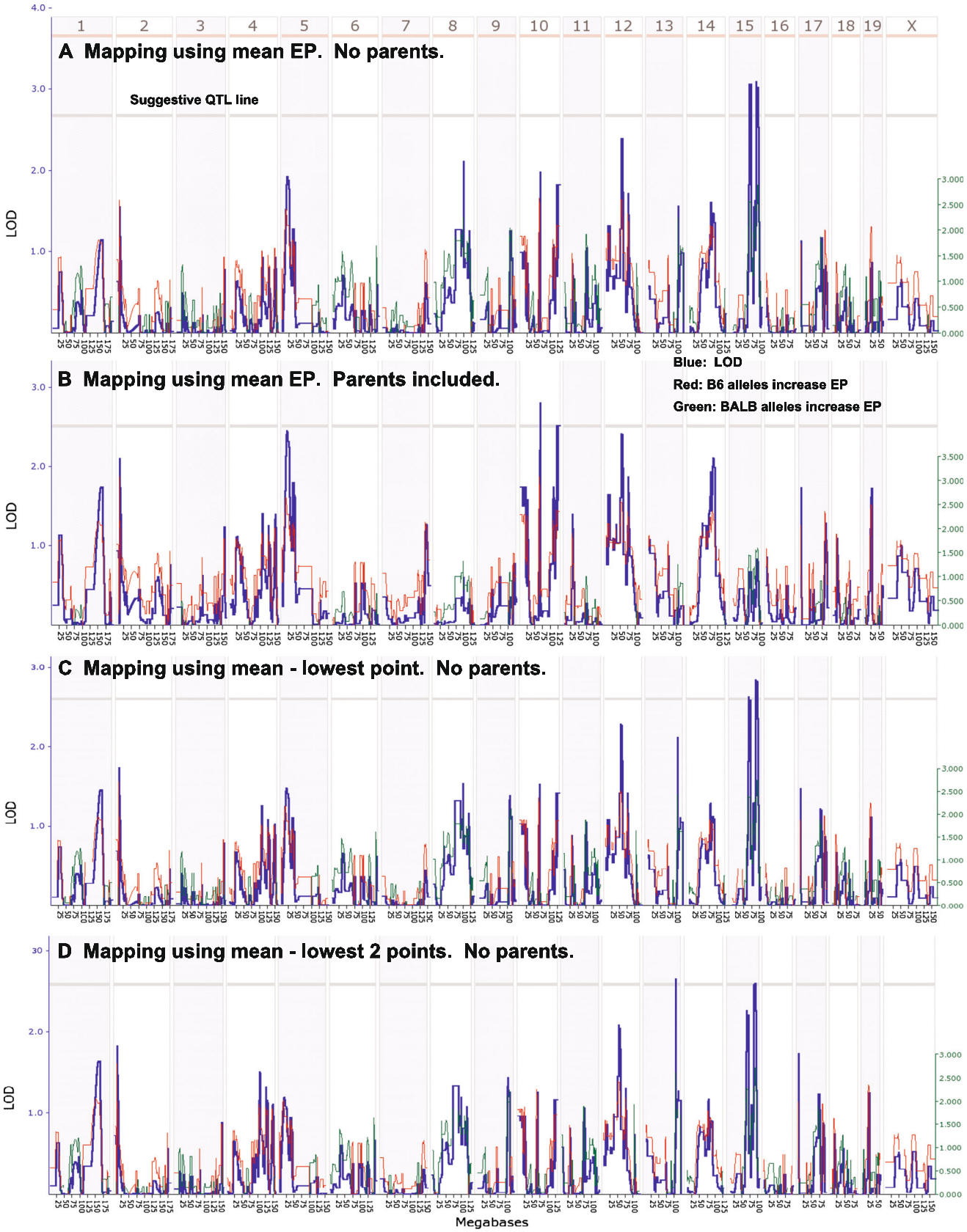
A Mapping using mean EP. No parents.
Suggestive QTL line
B Mapping using mean EP. Parents included.
Blue: LOD
Red: B6 alleles increase EP
Green: BALB alleles increase EP
C Mapping using mean - lowest point. No parents.
D Mapping using mean - lowest 2 points. No parents.
LOD
Megabases

span (from ~78–91 Mb). Five known genes meeting criteria lie at the peak of the first region (Tables S1 and 2). Among these, otoconin 90 (*Oc90*) is required for vestibular otoconial development (Yang et al. 2011). No relation to strial or lateral wall function has been shown, but some broader function in Ca^{++} homeostasis is possible. Cochlear lateral wall function involves a wide range of K^{+} channels, some with binding affinity or sequence similarity to *Kcnq3* (Holt and Corey 1999). However, we found no evidence in the literature for a significant role for this channel in lateral wall function. Thyroglobulin (*Tg*) modulates the expression of Pendrin (Royaux et al. 2000), which is required for lateral wall function. Many polymorphic genes lie within the more distal suggestive region. Among these, *Sox10* is required for the development and proper migration of neural crest

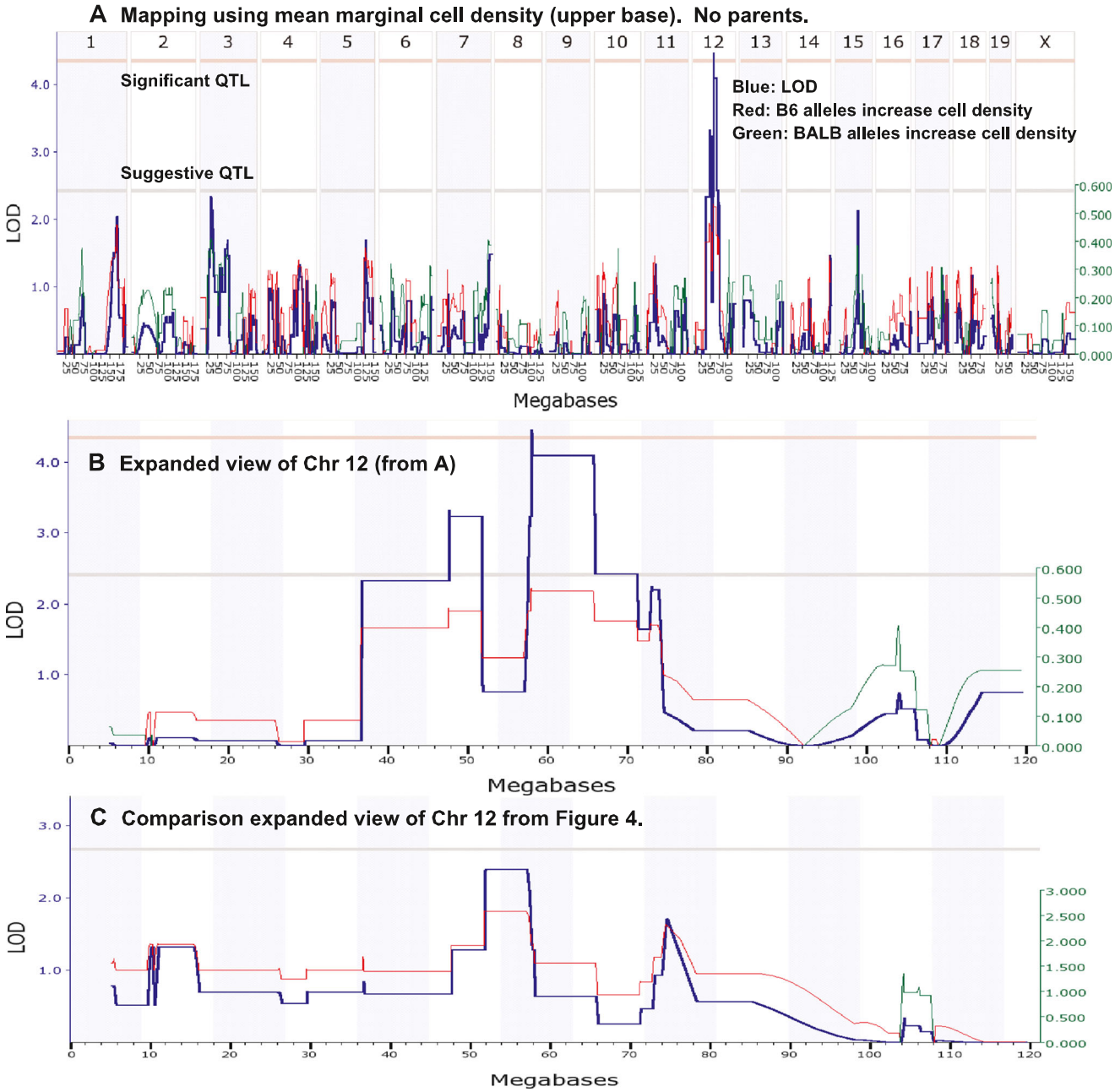

FIG. 5. **A** QTL map for mean strial marginal cell density generated using WebQTL, taken directly from the GeneNetwork website. **B, C** Comparison of QTL maps for strial marginal cell density (**B**) and EP (**C**) for chromosome 12 alone. Map for EP is an expansion of data for chromosome 12 in Figure 4A. The two maps overlap, although peak LOD scores do not correspond. *Colored traces* and *Y* axes have same meaning as in Figure 4.

cells, including strial intermediate cells (Watanabe et al. 2000), and has been implicated in how aging affects the stria (Hao et al. 2014). *Kcnj4* encodes a K^+ channel, although with no established role in lateral wall function (Alsaber et al. 2006). Like *Sox10*, *Atf4* is involved in the development and migration of neural crest cells (Dunn et al. 2000).

Strain distribution of acute CAP thresholds and EPs in noise-exposed mice

Acute effects of noise exposure on CAP thresholds were inferred by comparing means in exposed and unexposed mice. In the hours after noise, strains exhibited highly variable threshold elevations at the lowest frequencies and 40–90 dB at 10–20 kHz, the region of maximum sensitivity (Fig. 1). While animals with low post-noise EPs had higher thresholds (Fig. 6), most acute threshold elevation was not accompanied by EP changes. This is not surprising, since noise imposes a number of other types of injury that mostly affect the organ of Corti (e.g., Nordmann et al. 2000; Wang et al. 2002). Overt breaches in the organ of Corti, which might directly link organ of Corti injury and EP reduction (Salt and Konishi 1979; Hirose and Liberman 2003), appear infrequent in BALBs under the exposure conditions used here (Ohlemiller et al. 2011). Although strain variation in the effects of noise on thresholds at mid- and high-frequencies likely reflect multiple susceptibility factors, more straightforward effects of an acute EP change might be observed at lower frequencies. Figure 1 shows some low-frequency (2.5–5 kHz) threshold trends that might be predicted from acute EP changes. The strains for which the EP was most severely and consistently reduced (BALB and CxB4, Fig. 1B and G) showed the largest acute threshold shifts at low frequencies. Also, strains where, as we show, the EP tended to increase after noise (CxB3 and CxB8, Fig. 1F and K) exhibited among the smallest threshold shifts at low frequencies. Some other strains (most notably CxB7, Fig. 1J) did not fit this pattern, however.

QTLs for acute noise-related EP changes

Acute noise-related EP changes are depicted in Figure 7. In the raw scatterplot of Figure 7A, data from strains that showed significant EP changes by *t* test are enclosed in boxes. Figure 7B collapses strain data to averages to facilitate comparison by condition. Only one strain (CxB4) exhibited acute EP reduction approaching that in the BALB parent strain, and only one additional strain (CxB5) showed significant reduction. For an *EP-reduction* phenotype to manifest in only 2 of 12 RI strains (17 %)—neither

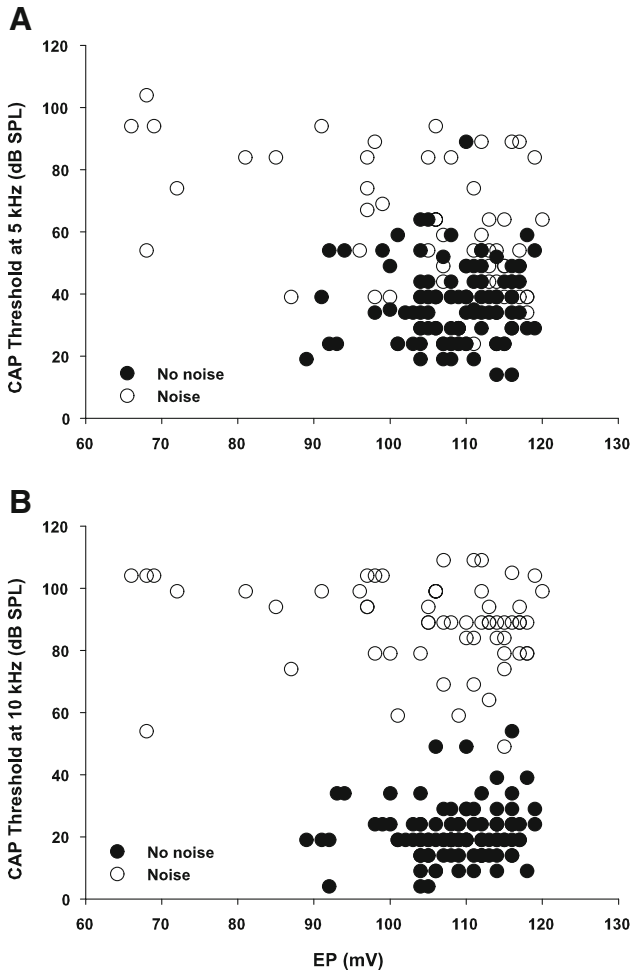

FIG. 6. Scatter plot comparison of CAP thresholds before and after noise at 5 kHz (**A**) and 10 kHz (**B**). Most threshold elevations did not coincide with EP reduction.

of which completely recapitulate the BALB phenotype—suggests that EP reduction in BALBs reflects the contribution of multiple recessive alleles, relative to B6. Every contributing allele should be fixed in roughly half the strains. Thus, three contributing alleles might be fixed in $(0.5)^3$, or 13 % of the strains. These may contribute unevenly and be nonlinear in their combinatorial effects. Their effects might also be mitigated by alleles that increase the EP after noise. Two strains (CxB3, CxB8) showed modest but significant EP increases after noise. While EP reductions may reflect lateral wall pathology, acute EP increase are suggested to reflect changes in the K^+ permeability of the organ of Corti (Konishi et al. 1979; Salt and Konishi 1979), so that different types of genes and expression patterns may underlie these opposing effects. In Table 3 we therefore consider genes in both lateral wall and organ of Corti, while restricting discussion to the most plausible candidates within four sugges-

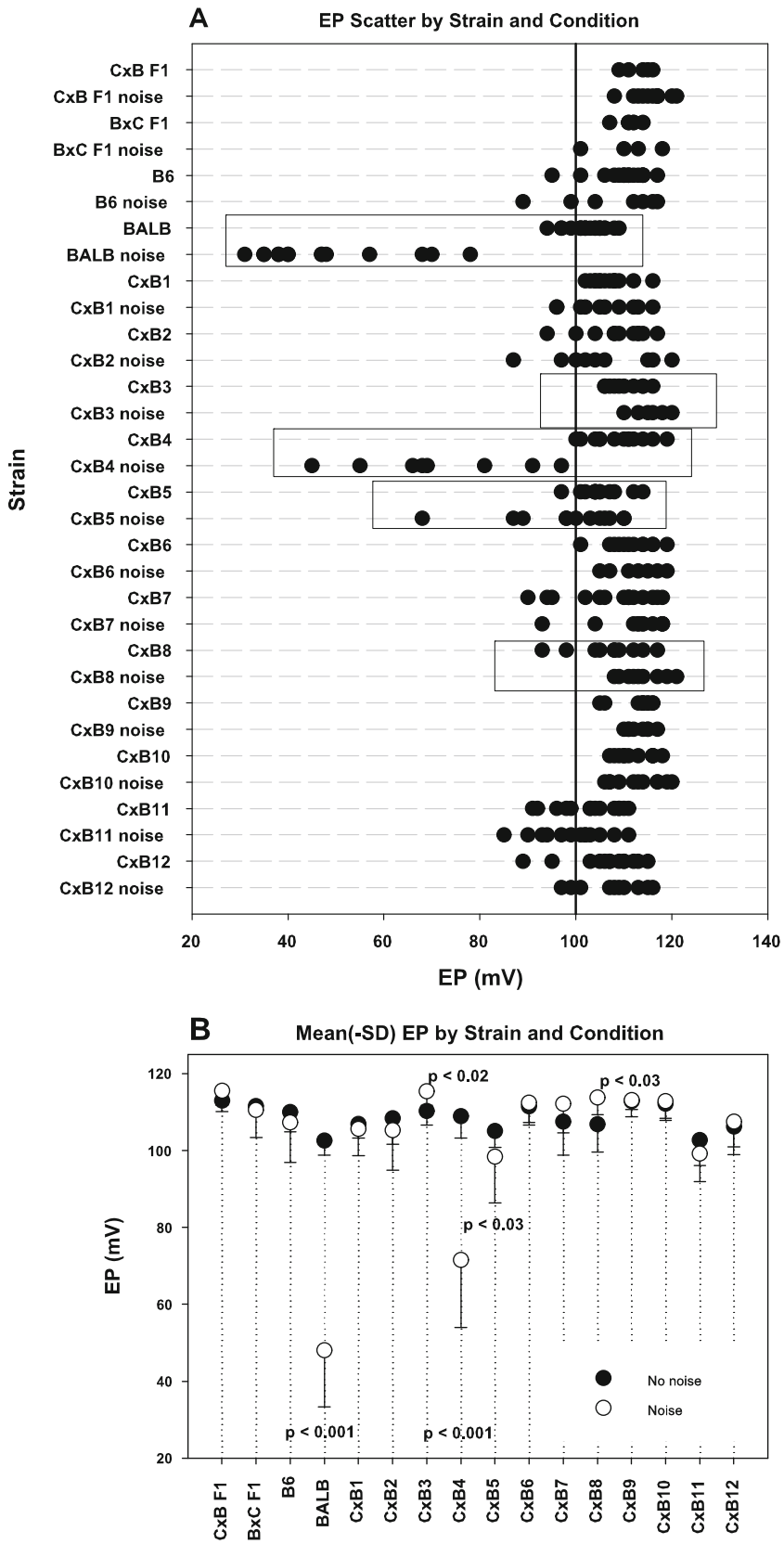

FIG. 7. **A** Scatter plot of EPs with, and without, noise in B6, BALB, F1 hybrids, and RI strains. Significant differences within strain as indicated by *t* test are enclosed by boxes. Two RI strains (CxB4, CxB5) showed significant acute EP reduction by noise. Two RI strains (CxB3, CxB8) showed significant EP increases. **B** Acute effect of noise on mean EP (−standard deviation) by strain with results of *t* tests.

tive intervals. Table S2 is much more inclusive, encompassing genes in most visually discernible peaks from Figure 8.

Chromosome 5

Proximal chromosome 5 showed two narrow peaks extending from ~3-41 Mb (Fig. 8, Table S2). For one or more genes in this region, B6 alleles act to increase the EP post-noise. Only the most proximal peak was suggestive, but we consider them together here, since the QTL in this general region mapped in CBA/J was extremely broad (Ohlemiller et al. 2010a). The peak LOD score in CBA/J occurred somewhat more distally (~48 Mb), but was based on only three markers. Ten genes met criteria for location, polymorphic character, and functional

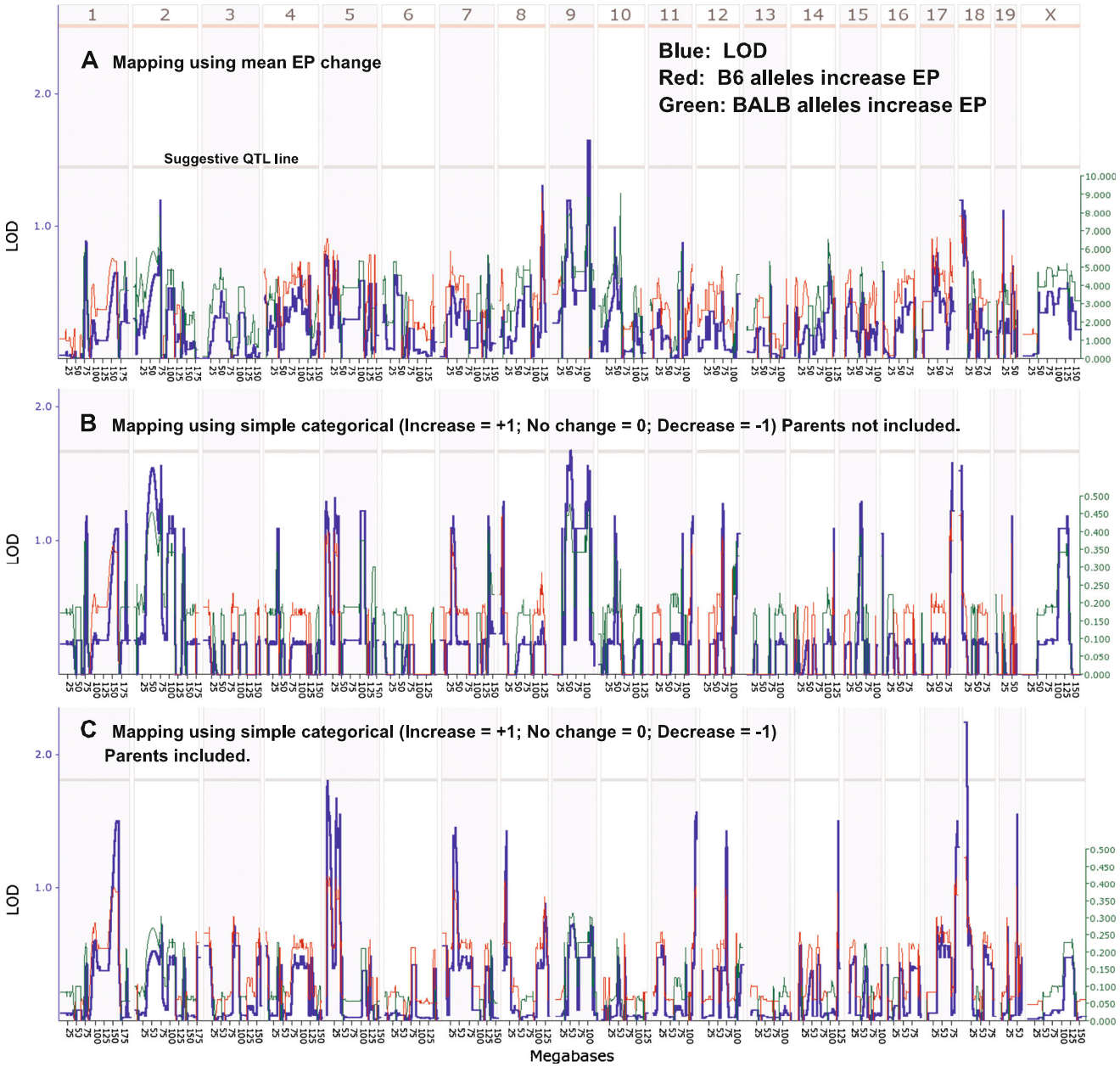

FIG. 8. QTL maps for mean EP in noise-exposed mice generated using WebQTL. Plots are taken directly from the GeneNetwork website. Three mapping strategies were compared, depending upon whether parent strain data were used, and whether mapping was based on mean EP change by group (**A**), or categorical (**B**, **C**), wherein a significant reduction was scored −1, no change was scored 0, and a significant increase was scored +1. Similar QTL regions recurred in multiple maps, although LOD scores depended on mapping strategy. *Blue traces* indicate LOD scores by chromosome (*left Y axis*), while *red* and *green traces* (additive effects, *right Y axis*) respectively indicate regions where B6 or BALB alleles tended to increase the EP (see Tables S2 and 3). Significance of LOD scores (*horizontal lines*, see text) was determined by WebQTL.

relatedness (Table 3). Among these, *Akap9* (*Yotiao*) encodes the A-kinase anchor protein-9, which engages the KCNQ1 binding domain and coordinates the phosphorylation state of this ion channel, and potentially the activity of the KCNQ1/KCNE1 complex (Summers et al. 2010). *Emilin1* encodes a protein that binds to Cnga1 at the tips of hair cell stereocilia (Selvakumar et al. 2012) and could affect current sinking by noise-damaged stereocilia and the current load on the stria. Mpv17 and related proteins localize to lysosomes and appear to play a critical role in maintaining stria vascularis (Meyer zum Gottesberge et al. 2012). *Wfs1* (*DFNA38*) encodes wolframin, an endoplasmic reticulum transmembrane protein expressed in many cell types, including sensory and non-sensory cells in the cochlea (Cryns et al. 2003). *Wdr1* (WD40 repeat domain) shows noise-modulated expression in both organ of Corti and lateral wall (Oh et al. 2002), and has been proposed to serve a protective role. Several genes in the region (*Fzd1, Shh, Hmx1, Otop1*) appear in the cochlear literature primarily for their role in development (Riccomagno et al. 2002; Wang and Lufkin 2005; Hughes et al. 2006; Bohnenpoll et al. 2014), yet may participate in responses to stress. If allelic similarity between B6, BALB, and CBA/J can serve as a guide, we may particularly suspect genes that are similar between BALB and CBA/J, yet polymorphic between these strains and B6. As Table 3 shows, this analysis would favor *Shh, Emilin1, Mpv17, Hmx1, Wfs1, Otop1*, or *Wdr1*.

Chromosome 9

Chromosome 9 features mid- and distal regions where BALB alleles act to increase the EP. Mapping in CBA/J mice produced no QTLs on this chromosome. Genes in these regions that met criteria include *Ncam1*, which encodes a cell adhesion molecule shown to be down-regulated in the lateral wall of noise-exposed rats (Cai et al. 2012). *Hspb2* encodes a protective heat shock protein, albeit one not well described in the cochlea (Leonova et al. 2002). *Cryab* (Alpha B crystalline) encodes a protein shown to be differentially expressed in *noise-resistant* and *vulnerable* mouse strains (Gratton et al. 2011). *Rdx* encodes radixin, a protein required for mechanical integrity of hair cell stereocilia (Kitajiri et al. 2004). Radixin could elevate the EP by reducing the current-sinking ability of noise-traumatized hair bundles. *Elmod1* is likewise involved in the development of stereocilia (Johnson et al. 2012), and could play a similar role. *Cyp19a1* mediates aromatization of androgens into estrogens, and was shown to modulate noise-induced hearing loss (Meltser et al. 2008). *Tmie* (*DFNB6*) has been implicated in hair cell transduction (Mitchem et al. 2002). Thus, at least three candidate genes on chromosome 9 (*Rdx, Elmod1, Tmie*) could increase the EP through an influence on hair cell transduction and K^+ permeability of the organ of Corti.

Chromosome 18

The QTL region on chromosome 18 appears restricted to a much more proximal region than the peak span encompassed by *Nirep* in CBA/J mice (~10 Mb versus ~65 Mb) (Ohlemiller et al. 2010a). The earlier mapping effort was limited by sample size and marker density, so that the narrower region seen in BALBs may be a refinement, or it may indicate that at least partly different genes on proximal chromosome 18 underlie the very similar CBA/J and BALB noise phenotypes. Because the BALB QTL region is relatively small, Table 3 lists some polymorphic genes for which no cochlear role is established. Among candidates, *Zeb1* is a transcription factor strongly expressed in spiral ligament (Hertzano et al. 2011). One of its actions is downregulation of Cx26, a previously claimed effect of noise exposure that could depress the EP and potentially amplify injury to the organ of Corti (Nagashima et al. 2010). *Arhgap12*, another Rho-GTPase activator, was recently described in the inner ear (Rudnicki et al. 2014). It is broadly expressed in the cochlea, mostly localized to epithelial cell-cell junctions. *Armc4* is implicated in ciliary development and ciliopathy (Hjeij et al. 2013), although no cochlear connection has been shown. *Mpp7* appears involved in epithelial tight junction formation (Xiao et al. 2012), although again, no close cochlear link has been described. *Gjd4* encodes a gap junctional component (Cx39) that has not been described in the cochlea (Oyamada et al. 2013). Once again, if allelic similarity between B6, BALB, and CBA/J provides a guide, we may suspect genes that are similar between BALB and CBA/J, and polymorphic between these strains and B6. This analysis favors *Crem, Arhgap12, Armc4, Mpp7, Gjd4, Greb1l*, and *Gata6* (Table 3).

DISCUSSION

The present study provides new evidence that genetic variance gives rise to EP variance, with or without noise, and suggests novel genes (and gene types) that may be involved. By and large, the pool of suggested candidates does not include major genes known to be critical for EP generation. Instead, most of the candidates appear modulatory, developmentally related, or stress-related.

Limitations

A number of caveats attend our findings. The power of RI strains for QTL mapping depends on the number of strains in the RI series used. We were constrained to use a comparatively small series (12 of 13 commercially available CxB strains). The result was a moderate number of

statistically marginal QTL intervals on several chromosomes. Some of these may be false positives, deriving from the strain distribution pattern of wholly unrelated phenotypes that are fortuitously isomorphic with EP. Because of the organ of Corti focus of most genetic hearing studies, presently little is known of the genes that might subtly influence the EP. This makes it more difficult to suggest which genes in any QTL interval are most likely to be relevant. Genes we did not emphasize from Tables S1 and S2 may in time prove more critical than those in Tables 2 or 3, leading to quite different genetic models of EP variance. Our analysis also emphasized conventional genes. We did not consider genes encoding regulatory RNAs. To limit the sheer number of candidates, in assessing polymorphisms, we ignored those downstream or within introns unless a splice site was impacted.

Our work implicitly addresses age-associated strial pathology, yet we did not examine old animals. Rather, this work proceeds from the premise that early, genetically determined differences may predispose some mouse lines to age-associated EP decline. Hence, we would predict from Figure 2 that the CxB strains located closest to BALBs on the *x* axis would be most likely to exhibit EP decline with aging, but this is untested.

Finally, genes implicated in this work may only apply to B6-versus-BALB and CBA/J EP differences. They may not ultimately be found to account for differences versus other inbred strains, across mammalian species, or across human populations. Nevertheless, these findings constitute an important first step into a near void of information about genetically modulated EP variation and its consequences for hearing across the lifespan. More comparative studies will be required to test reproducibility of QTLs we identify, and to sort through candidate genes.

Genes and processes that establish or modulate the EP

Major requirements for a normal EP are well studied (Wangemann 2006; Nin et al. 2008; Hibino et al. 2010). These include a source of K^+, ion-tight boundaries surrounding scala media and the stria itself, a three-cell-layered composition of the stria, and a stoichiometrically appropriate complement of pumps, exchangers, and channels that include Na^+/K^+ATPase, NKCC1, KCNE1/KCNQ1, and KCNJ10. A large outward flux of K^+ across KCNJ10 in strial intermediate cells is thought to represent the single indispensable event in EP generation. It may be advantageous if there are control mechanisms for modulating the EP. This may help match stria *source* and organ of Corti *load*, or may be protective during noise exposure. Mechanisms that may have evolved for downregulating the EP include purinergic modulation of the conductance of KCNQ1/KCNE1 (Mockett et al. 1994; Lee et al. 2001) and also a feed-forward loop whereby ATP released by the stria opens K^+ shunt conductances (Housley et al. 2013). Genetic disruption of the proper ratio of Na^+/K^+ATPase to NKCC1 activity in strial marginal cells reduces the EP (Diaz et al. 2007). Marginal cell dysfunction or loss constitutes the most general anatomic correlate of strial presbycusis (Schuknecht et al. 1974; Spicer and Schulte 2005; Ohlemiller 2009), and appears to be a characteristic of some genetic strial pathologies (e.g., Kim et al. 2014). It is not asserted that this creates leaky patches of stria lacking any marginal cells. Rather, the luminal face of the stria becomes covered by fewer, larger marginal cells that may express too little of one or more K^+ transport components. Mutations that promote large-scale hair cell loss and scar formation (Bryda et al. 2012) or chronically decrease K^+ flux through hair cells (Nie et al. 2006) have been associated with especially high EPs in mice. Thus, a high standing EP does not necessarily point to processes that are beneficial for hearing, but rather may reflect impaired hair cell survival and function.

Given the impracticality and nonsystematic character of human EP recordings, we cannot be certain which of the above circumstances apply clinically. It is encouraging, however, that the single thread unifying human and animal observations in strial presbycusis (the limiting nature of strial marginal cells) corresponds to our identification of *Maced* as a locus that may jointly impact EP and marginal cell density. The young BALB stria vascularis may not manifest obvious pathology, nor generate a clearly abnormal EP, owing perhaps to the functional redundancy of the stria (Ohlemiller 2009). However, BALB marginal cells may begin life compromised in function and viability, leading also to accelerated dropout and further spreading of the surviving cells. Since the highest EPs were observed in the F1 hybrids (Fig. 2), and since the extent of any organ of Corti pathology that might elevate the EP is expected to be similar in B6 and BALB mice, *EP elevating* QTLs in Table 2 may hold advantageous alleles of genes expressed within the lateral wall. The list of polymorphic genes in the *Maced* interval, where B6 mice appear to carry beneficial alleles, includes several potentially relevant genes. Particularly interesting among these are *Foxg1, Foxa1, Akap6, Nkx2-1, and Pax9*. Notable lateral wall genes in the other QTL regions include *Sirt1, Ddit3/CHOP, Lrp1, Kcnq3, Tg, Sox10, Kcnj4,* and *Atf4*.

Genes and processes that may increase or decrease the EP after noise

Depending upon RI strain, the EP either decreased or increased acutely after noise (Fig. 7). Several investigators have reported EP reductions in animals after noise (Melichar et al. 1980; Vassout 1984; Ikeda et al. 1988; Ahmad et al. 2003; Hirose and Liberman

2003; Ohlemiller and Gagnon 2007; Ohlemiller et al. 2010a, 2011), and EP reductions were the original impetus for our mapping efforts in noise-exposed mice. Reports of acute EP increase after noise are fewer (Konishi et al. 1979; Salt and Konishi 1979; Wang et al. 1992), leading to disagreement over when and how these may occur. One immediate implication of the present data is that disparate findings over the *direction* of EP change may have their origins not only in the conditions tested, nor only in the species examined, but in the precise genetic background within species. Regardless of any implications for NIPTS, the contribution of EP changes to acute threshold shifts in different model systems may vary qualitatively.

Based on our previous work in B6, CBA/J, and BALB mice, EP reductions caused by the type of noise we applied reflect lateral wall pathology. Specific cell pathologies of stria and spiral ligament were significantly correlated with EP, and little evidence for discontinuities within the reticular lamina was found. Hence, we anticipate that the genes we seek to account for acute EP reduction are expressed primarily in the lateral wall. It is not clear how and why over-driving the organ of Corti with noise should damage the stria and ligament. For 2-h, 110 dB exposures, acute cellular pathology (as viewed by light microscope) is wide-spread, encompassing most fibrocyte types, strial basal cells, and even Reissner's membrane. It is not known whether or how the stria *senses* organ of Corti K^+ flux or metabolic demand, or whether the pathology we find reflects an attempt to compensate. Efficient removal of excess K^+ from the organ of Corti requires active pumping by type II fibrocytes in inferior spiral ligament, possibly explaining the appearance of these cells, and potentially depriving the stria of K^+. Yet this need not promote overt strial pathology. Notably, mitochondrial inhibitors applied in guinea pigs reproduce many of the features of noise injury (Hoya et al. 2004; Okamoto et al. 2005), while gap junction inhibitors only somewhat reproduce the effects of noise (Spiess et al. 2002). In any event, the appearance of the lateral wall does not readily indicate which cells or genes may drive phenotypic differences. It is nevertheless reassuring that both BALB and CBA/J EP-reduction phenotypes point to overlapping QTLs on chromosomes 5 and 18 (Ohlemiller et al. 2010a), and that B6 alleles in these regions increase EP values. Particularly suitable gene candidates on chromosome 5 include *Akap9, Mpv17*, and *Wdr1*. It cannot be ruled out that the present mapping data for chromosome 18 subdivide the *Nirep* QTL into two regions that each contribute to similar noise phenotypes in BALB and CBA/J. The present map restricts this region to the most proximal ~11 Mb, while our earlier map extended >60 Mb. Intriguing gene candidates in the more restricted interval include *Zeb1, Arhgap12, Mpp7,* and *Gjd4*.

Two RI strains showed EP increases after noise (Fig. 7). Mapped QTLs (Tables S2 and 3) include two regions on chromosome 9 where BALB alleles that increase the EP emerged when parental data were omitted (Fig. 8A, B). Previous demonstrations of EP increases by noise attributed this to reduced K^+ permeability of the organ of Corti (Konishi et al. 1979; Salt and Konishi 1979). The two regions of chromosome 9 may therefore hold unmasked BALB alleles that either protect the function of the lateral wall or reduce K^+ flux through the organ of Corti. The latter could occur though impaired transduction, prolonged hair cell depolarization, or decreased K^+ leakage around hair cells. Such leakage is normally minimized by tight junctions that line cell-cell junctions of the reticular lamina. Elimination of tight junction proteins vezatin, claudin-9, claudin-14, occludin, angulin-2 (Ildr1), or tricellulin promotes hearing loss in mice (Ben-Yosef et al. 2003; Bahloul et al. 2009; Nakano et al. 2009; Nayak et al. 2013; Kitajiri et al. 2014; Morozko et al. 2014). In the case of claudins-9 and -14, in vitro recordings have shown that the junctions become leaky, likely allowing K^+ to enter the organ of Corti and potentially killing hair cells through K^+ toxicity. There is little evidence, however, tying compromised tight junctional proteins within the reticular lamina to EP reduction (but see Kazmierczak et al. 2015). The EP appears to be sensitive only to large changes in the ion-tightness of the reticular lamina, or to overt tears as may be caused by more intense noise than we applied (Salt and Konishi 1979; Melichar et al. 1980; Hirose and Liberman 2003). Therefore, the genes on chromosome 9 that favor acute noise-related increases in the EP likely encode components of the transduction apparatus. Strong candidates include *Rdx*, *Elmod1*, and *Tmie*. Other plausible types of genes include *Ncam1*, *Hspb2, Cryab*, and *Cyp19a1*.

Potential correlation of EP with other traits

The features of WebQTL include comparison of any numeric phenotype with published phenotypes, using Pearson or Spearman rank correlations. This allows investigators to consider whether their phenotype of interest may be related to other phenotypes through the involvement of overlapping genes or pathways. Such correlations need not be causal, and will often be coincidental. We compared Spearman rank correlations between the EP in our noise-exposed and non-exposed

mice and 100 other published phenotypes in CxB mice and their parent strains. For the non-exposed condition, we simply used mean EP by strain (Fig. 2). WebQTL identified 10 traits that are significantly correlated ($p < 0.05$), some of which involve inflammation or cancer susceptibility. None of these mapped to regions detailed in Table 2. For the noise-exposed condition, we tested both mean EP change and mean post-noise EP. Mean EP change (as mapped in Fig. 8) netted 45 significant correlations. Interestingly, the top five correlations all involve plasma cholesterol or serum or tissue thyroxine (see Table S3). The only genetic overlap with the present mapping data is a common span of distal chromosome 9 that holds a QTL for serum thyroxine. Spearman rank analysis for mean EP after noise revealed 37 significant correlations for widely divergent traits, yet cholesterol and thyroxin again comprised two of the top three. Both cholesterol and thyroxine regulation have been implicated in cochlear function and susceptibility to injury (Kohonen et al. 1971; Berndt and Wagner 1979; Axelsson and Lindgren 1985; Crumling et al. 2012). It is thus possible that some common genes or downstream cascades involving these partly mediate noise-related EP changes.

ACKNOWLEDGMENTS

We thank Drs. R.J. Morell (NIDCD) and A.N. Salt (WUSM Dept. Otolaryngology) for comments on the manuscript. Thanks also to Drs. K.R. Johnson (JAX) and R.W. Williams (U. Tennessee Health Sciences Center) for helpful discussions.

COMPLIANCE WITH ETHICAL STANDARDS

Funding Agencies Supported by NIH R01 DC03454 and DC08321 (KKO), P30 DC04665 (R. Chole), NIH T35 DC008765 (W.W. Clark), and Washington University Medical School Department of Otolaryngology.

REFERENCES

Abraira VE, Satoh T, Fekete DM, Goodrich LV (2010) Vertebrate Lrig3-ErbB interactions occur in vitro but are unlikely to play a role in Lrig3-dependent inner ear morphogenesis. PLoS One 5, e8981

Adams JC (2009) Immunocytochemical traits of type IV fibrocytes and their possible relations to cochlear function and pathology. J Assoc Res Otolaryngol 10:369–382

Ahmad M, Bohne BA, Harding GW (2003) An in vivo tracer study of noise-induced damage to the reticular lamina. Hear Res 175:82–100

Alsaber R, Tabone C, Kandpal R (2006) Predicting candidate genes for human deafness disorders: a bioinformatics approach. BMC Genomics 7:180

Axelsson A, Lindgren F (1985) Is there a relationship between hypercholesterolemia and noise-induced hearing loss? Acta Otolaryngol 100:379–386

Bahloul A, Simmler M-C, Michel V, Leibovici M, Perfettini I, Roux I, Weil D, Nouaille S, Zuo J, Zadro C, Licastro D, Gasparini P, Avan P, Hardelin J-P, Petit C (2009) Vezatin, an integral membrane protein of adherens junctions, is required for the sound resilience of cochlear cells. EMBO Mol Med 1:125–138

Bell D, Streit A, Gorospe I, Varela-Nieto I, Alsina B, Giraldez F (2008) Spatial and temporal segregation of auditory and vestibular neurons in the otic placode. Dev Biol 322:109–120

Ben-Yosef T, Belyantseva IA, Saunders TL, Hughes ED, Kawamoto K, Van Itallie CM, Beyer LA, Halsey K, Gardner DJ, Wilcox ER, Rasmussen J, Anderson JM, Dolan DF, Forge A, Raphael Y, Camper SA, Friedman TB (2003) Claudin 14 knockout mice, a model for autosomal recessive deafness DFNB29, are deaf due to cochlear hair cell degeneration. Hum Mol Genet 12:2049–2061

Berndt H, Wagner H (1979) Influence of thyroid state and improved hypoxia tolerance on noise-induced cochlea damage. Eur Arch Otorhinolaryngol 224:125–128

Bohnenpoll T, Trowe M-O, Wojahn I, Taketo MM, Petry M, Kispert A (2014) Canonical Wnt signaling regulates the proliferative expansion and differentiation of fibrocytes in the murine inner ear. Dev Biol 391:54–65

Braunstein EM, Monks DC, Aggarwal VS, Arnold JS, Morrow BE (2009) Tbx1 and Brn4 regulate retinoic acid metabolic genes during cochlear morphogenesis. BMC Dev Biol 9:31

Bryda EC, Johnson NT, Ohlemiller KK, Besch-Williford CL, Moore E, Bram RJ (2012) Conditional deletion of calcium-modulating cyclophilin ligand causes deafness in mice. Mamm Genome 23:270–276

Cai Q, Patel M, Coling DE, Hu BH (2012) Transcriptional changes in adhesion-related genes are site-specific during noise-induced cochlear pathogenesis. Neurobiol Dis 45:723–732

Chaplin JW, Kasahara S, Clark EA, Ledbetter JA (2009) CD180 is a positive regulator of TLR signals in B cells. J Immunol 182:135–164

Chatterjee S, Kraus P, Lufkin T (2010) A symphony of inner ear developmental control genes. BMC Genet 11:68

Cirillo LA, Zaret KS (2007) Specific interactions of the wing domains of FOXA1 transcription factor with DNA. J Mol Biol 366:720–724

Conlee JW, Abdul-Baqi KJ, McCandless GA, Creel DJ (1986) Differential susceptibility to noise-induced permanent threshold shift between albino and pigmented guinea pigs. Hear Res 23:81–91

Conlee JW, Abdul-Baqi KJ, McCandless GA, Creel DJ (1988) Effects of aging on normal hearing loss and noise-induced threshold shift in albino and pigmented guinea pigs. Acta Otolaryngol 106:64–70

Crumling MA, Liu L, Thomas PV, Benson J, Kanicki A, Kabara L, Halsey K, Dolan DF, Duncan RK (2012) Hearing loss and hair cell death in mice given the cholesterol-chelating agent hydroxy-propyl-beta-cyclodextrin. PLoS One 7:12

Cryns K, Thys S, Van Laer L, Oka Y, Pfister M, Van Nassauw L, Smith RJH, Timmermans J-P, Van Camp G (2003) The WFS1 gene, responsible for low frequency sensorineural hearing loss and Wolfram syndrome, is expressed in a variety of inner ear cells. Histochem Cell Biol 119:247–256

Diaz RC, Vazquez AE, Dou H, Wei D, Cardell EL, Lingrel J, Shull GE, Doyle KJ, Yamoah EN (2007) Conservation of hearing by simultaneous mutation of Na, K-ATPase and NKCCl. J Assoc Res Otolaryngol 8:422–434

Diviani D, Maric D, López IP, Cavin S, del Vescovo CD (2013) A-kinase anchoring proteins: molecular regulators of the cardiac

stress response. Biochim Biophys Acta Mol Cell Res 1833:901–908

Dong H, Zhang P, Song I, Petralia RS, Liao D, Huganir RL (1999) Characterization of the glutamate receptor-interacting proteins GRIP1 and GRIP2. J Neurosci Methods 19:6930–6941

Dunn KJ, Williams BO, Li Y, Pavan WJ (2000) Neural crest-directed gene transfer demonstrates Wnt1 role in melanocyte expansion and differentiation during mouse development. Proc Natl Acad Sci U S A 97:10050–10055

Duvall AJ, Ward WD, Lauhala KE (1974) Stria ultrastructure and vessel transport in acoustic trauma. Ann Otol Rhinol Laryngol 83:498–514

Erway LC, Willott JF, Archer JR, Harrison DE (1993) Genetics of age-related hearing loss in mice: I. Inbred and F1 hybrid strains. Hear Res 65:125–132

Fujinami Y, Mutai H, Kamiya K, Mizutari K, Fujii M, Matsunaga T (2012) Enhanced expression of C/EBP homologous protein (CHOP) precedes degeneration of fibrocytes in the lateral wall after acute cochlear mitochondrial dysfunction induced by 3-nitropropionic acid. Neurochem Int 56:487–494

Furukawa Y, Kawasoe T, Daigo Y, Nishiwaki T, Ishiguro H, Takahashi M, Kitayama J, Nakamura Y (2001) Isolation of a novel human gene, ARHGAP9 encoding a Rho-GTPase activating protein. Biochem Biophys Res Commun 284:643–649

Garland P, Quraishe S, French P, O'Connor V (2008) Expression of the MAST family of serine/threonine kinases. Brain Res Rev 1195:12–19

Gratton MA, Eleftheriadou A, Garcia J, Verduzco E, Martin GK, Lonsbury–Martin BL, Vázquez AE (2011) Noise-induced changes in gene expression in the cochleae of mice differing in their susceptibility to noise damage. Hear Res 2011:211–226

Han F, Zhang H, Gu L (2005) Expression and its significance of aquaporins in normal guinea pig inner ears. J Clin Otorhinolaryngol 19:10

Hao X, Xing Y, Moore MW, Zhang J, Han D, Schulte BA, Dubno JR, Lang H (2014) Sox10 expressing cells in the lateral wall of the aged mouse and human cochlea. PLoS One 9, e97389

Hertzano R, Elkon R, Kurima K, Morrisson A, Chan S-L, Sallin M, Biedlingmaier A, Darling DS, Griffith AJ, Eisenman DJ, Strome SE (2011) Cell type-specific transcriptome analysis reveals a major role for Zeb1 and miR-200b in mouse inner ear morphogenesis. PLoS One 7, e1002309

Hibino H, Nin F, Tsuzuki C, Kurachi Y (2010) How is the highly positive endocochlear potential formed? The specific architecture of the stria vascularis and the roles of the ion-transport apparatus. Pflugers Arch Eur J Physiol 459:521–533

Hirose K, Liberman MC (2003) Lateral wall histopathology and endocochlear potential in the noise-damaged mouse cochlea. J Assoc Res Otolaryngol 4:339–352

Hitzemann R, Bell J, Rasmussen E, McCaughran J (2001) Chapter 21. Mapping the genes for the acoustic startle response (ASR) and prepulse inhibition of the ASR in the BxD recombinant inbred series: Effect of high-frequency hearing loss and cochlear pathology. In: Willott JF (ed) Handbook of mouse auditory research: from behavior to molecular biology. CRC Press, Boca Raton, pp 441–455

Hjeij R, Lindstrand A, Francis R, Zariwala MA, Liu X, Li Y, Damerla R, Dougherty GW, Abouhamed M, Olbrich H, Loges NT, Pennekamp P, Davis EE, Carvalho CMB, Pehlivan D, Werner C, Raidt J, Kohler G, Haffner K, Reyes-Mugica M, Lupski JR, Leigh MW, Rosenfeld M, Morgan LC, Knowles MR, Lo CW, Katsanis N, Omran H (2013) *ARMC4* mutations cause primary ciliary dyskinesia with randomization of left/right body asymmetry. Am J Med Genet 93:357–367

Holt JR, Corey DP (1999) Ion channel defects in hereditary hearing loss. Neuron 22:217–219

Housley GD, Morton-Jones R, Vlajkovic SM, Telang RS, Paramanthasivam V, Tadros SF, Wong ACY, Froud KE, Cederholm JME, Sivakumaran Y, Snguanwongchai P, Khakh BS, Cockayne DA, Thorne PR, Ryan AF (2013) ATP-gated ion channels mediate adaptation to elevated sound levels. Proc Natl Acad Sci U S A 110:7494–7499

Howard BA (2012) In the beginning: the establishment of the mammary lineage during embryogenesis. Semim Cell Dev Biol 23:574–582

Hoya N, Okamoto Y, Kamiya K, Fujii M, Matsunaga T (2004) A novel animal model of acute cochlear mitochondrial dysfunction. Neuroreport 15:1597–1600

Hughes I, Thalmann I, Thalmann R, Ornitz DM (2006) Mixing model systems: using zebrafish and mouse inner ear mutants and other organ systems to unravel the mystery of otoconial development. Brain Res 1091:58–74

Ide M, Morimitsu T (1990) Long term effects of intense sound on endocochlear DC potential. Auris Nasus Larynx 17:1–10

Ikeda K, Kusakari J, Takasaka T (1988) Ionic changes in cochlear endolymph of the guinea pig induced by acoustic injury. Hear Res 32:103–110

Johnson KR, Zheng QY, Erway LC (2000) A major gene affecting age-related hearing loss is common to at least 10 inbred strains of mice. Genomics 70:171–180

Johnson KR, Longo-Guess CM, Gagnon LH (2012) Mutations of the mouse ELMO domain containing 1 gene (Elmod1) link small GTPase signaling to actin cytoskeleton dynamics in hair cell stereocilia. PLoS One 7, e36074

Kang C, Tian C, SoÌnnichsen FD, Smith JA, Meiler J, George AL Jr, Vanoye CG, Kim HJ, Sanders CR (2008) Structure of KCNE1 and implications for how it modulates the KCNQ1 potassium channel. Biochemistry 47:7999–8006

Kazmierczak M, Harris SL, Kazmierczak P, Shah P, Starovoytov V, Ohlemiller KK, Schwander M (2015) Progressive hearing loss in mice carrying a mutation in Usp53. J Neurosci 35:15582–15598

Kim H-J, Oh G-S, Lee J-H, Lyu A-R, Ji H-M, Lee S-H, Song J, Park S-J, You Y-O, Sul J-D, Park C, Chung S-Y, Moon S-K, Lim DJ, So H-S, Park R (2011) Cisplatin ototoxicity involves cytokines and STAT6 signaling network. Cell Res 21:944–956

Kim KX, Sanneman JD, Kim H-M, Harbidge DG, Xu J, Soleimani M, Wangemann P, Marcus DC (2014) Slc26a7 chloride channel activity and localization in mouse Reissner's membrane epithelium. PLoS One 9, e97191

Kitajiri S-I, Fukumoto K, Hata M, Sasaki H, Katsuno T, Nakagawa T, Ito J, Tsukita S, Tsukita S (2004) Radixin deficiency causes deafness associated with progressive degeneration of cochlear stereocilia. J Cell Biol 166:559–570

Kitajiri S-I, Katsuno T, Sasaki H, Ito J, Furuse M, Tsukita S (2014) Deafness in occludin-deficient mice with dislocation of tricellulin and progressive apoptosis of the hair cells. Biology Open, BIO20147799Kobayashi T, Aslan A, Chiba T, Takasaka T, Sanna M (1996) Measurement of endocochlear DC potentials in ears with acoustic neuromas: a preliminary report. Acta Otolaryngol 116:791–795

Kohonen A, Jauhiainen T, Liewendahl K, Tarkkanen J, Kaimio M (1971) Deafness in experimental hypo- and hyperthyroidism. Laryngoscope 81:947–956

Konishi T, Salt AN, Hamrick PE (1979) Effects of exposure to noise on ion movement in guinea pig cochlea. Hear Res 1:325–342

Lee JH, Chiba T, Marcus DC (2001) $P2X_2$ receptor mediates stimulation of parasensory cation absorption by cochlear outer sulcus cells and vestibular transitional cells. J Neurosci 21:9168–9174

Leonova EV, Fairfield DA, Lomax MI, Altschuler RA (2002) Constitutive expression of Hsp27 in the rat cochlea. Hear Res 163:61–70

Melichar I, Syka J, Ulehlova L (1980) Recovery of the endocochlear potential and the K+ concentrations in the cochlear fluids after acoustic trauma. Hear Res 2:55–63

Meltser I, Tahera Y, Simpson EM, Hultcrantz M, Charitidi K, Gustafsson J-A, Canlon B (2008) Estrogen receptor B protects against acoustic trauma in mice. J Clin Investig 118:1563–1570

Meyer zum Gottesberge AM, Massing T, Hansen S (2012) Missing mitochondrial Mpv17 gene function induces tissue-specific delldeath pathway in the degenerating inner ear. Cell Tissue Res 347:343–356

Mitchem KL, Hibbard E, Beyer LA, Bosom K, Dootz GA, Dolan DF, Johnson KR, Raphael Y, Kohrman DC (2002) Mutation of the novel gene Tmie results in sensory cell defects in the inner ear of spinner, a mouse model of human hearing loss DFNB6. Hum Mol Genet 11:1887–1898

Mockett BG, Housley GD, Thorne PR (1994) Fluorescence imaging of extracellular purinergic sites and putative ecto-ATPase sites on isolated cochlear hair cells. J Neurosci 14:1692–1707

Morozko EL, Nishio A, Ingham NJ, Chandra R, Fitzgerald T, Martelletti E, Borck G, Wilson E, Riordan GP, Wangemann P, Forge A, Steel KP, Liddle RA, Friedman TB, Belyantseva IA (2014) ILDR1 null mice, a model of human deafness DFNB42, show structural aberrations of tricellular tight junctions and degeneration of auditory hair cells. Hum Mol Genet 24(3):609–624

Nagashima R, Yamaguchi T, Tanaka H, Ogita K (2010) Mechanism underlying the protective effect of tempol and N^{w}-Nitro-L-Arginine Methyl Ester on acoustic injury: possible involvement of c-Jun N-Terminal Kinase pathway and Connexin26 in the cochlear spiral ligament. J Pharmacol 114:50–62

Nagtegaal AP, Spijker S, Crins TTH, Borst JGG (2012) A novel QTL underlying early-onset, low-frequency hearing loss in BXD recombinant inbred strains. Genes Brain Behav 11:911–920

Nakano Y, Kim SH, Kim H-M, Sanneman JD, Zhang Y, Smith RJH, Marcus DC, Wangemann P, Nessler RA, Banfi B (2009) A claudin-9-based ion permeability barrier is essential for hearing. PLoS Genet 5, e1000610

Nayak G, Lee SI, Yousaf R, Edelmann SE, Trincot C, Van Itallie CM, Sinha GP, Rafeeq M, Jones SM, Belyantseva IA, Anderson JM, Forge A, Frolenkov G, Riazuuddin S (2013) Tricellulin deficiency affects tight junction architecture and cochlear hair cells. J Clin Investig 123:4036–4049

Nemoto M, Morita Y, Mishima Y, Takahashi S, Nomura T, Ushiki T, Shiroishi T, Kikkawa Y, Yonekawa H, Kominami R (2004) *Ahl3*, a third locus on mouse chromosome 17 affecting age-related hearing loss. Biochem Biophys Res Commun 324:1283–1288

Nie L, Xu T, Mo J, Zhang Y, Feng W, Vazquez AE, Morris K, Beisel K, Yamoah EN (2006) Molecular cloning and functional study of KCNQ4 channels in the mouse inner ear. FASEB J 20:A1368

Nin F, Hibino H, Doi KS, Suzuki T, Hisa Y, Kurachi Y (2008) The endocochlear potential depends on two K+ diffusion potentials and an electrical barrier in the stria vascularis of the inner ear. Proc Natl Acad Sci U S A 105:1751–1756

Noben-Trauth K, Zheng QY, Johnson KR (2003) Association of cadherin 23 with polygenic inheritance and genetic modification of sensorineural hearing loss. Nat Genet 35:21–23

Noben-Trauth K, Latoche JR, Neely HR, Bennett B (2010) Phenotype and genetics of progressive sensorineural hearing loss (Snhl1) in the LXS set of recombinant inbred strains of mice. PLoS One 5, e11459

Nordmann AS, Bohne BA, Harding GW (2000) Histopathological differences between temporary and permanent threshold shift. Hear Res 139:13–30

Oh SH, Adler HJ, Raphael Y, Lomax MI (2002) WDR1 colocalizes with ADF and actin in the normal and noise-damaged chick cochlea. J Comp Neurol 448:399–409

Ohlemiller KK (2002) Reduction in sharpness of frequency tuning but not endocochlear potential in aging and noise-exposed BALB/cJ mice. J Assoc Res Otolaryngol 3:444–456

Ohlemiller KK (2009) Mechanisms and genes in human strial presbycusis from animal models. Brain Res 1277:70–83

Ohlemiller KK, Gagnon PM (2007) Genetic dependence of cochlear cells and structures injured by noise. Hear Res 224:34–50

Ohlemiller KK, Lett JM, Gagnon PM (2006) Cellular correlates of age-related endocochlear potential reduction in a mouse model. Hear Res 220:10–26

Ohlemiller KK, Rice MR, Lett JM, Gagnon PM (2009) Absence of strial melanin coincides with age associated marginal cell loss and endocochlear potential decline. Hear Res 249:1–14

Ohlemiller KK, Rosen AD, Gagnon PM (2010a) A major effect QTL on chromosome 18 for noise injury to the mouse cochlear lateral wall. Hear Res 260:47–53

Ohlemiller KK, Dahl AR, Gagnon PM (2010b) Divergent aging characteristics in CBA/J and CBA/CaJ mouse cochleae. J Assoc Res Otolaryngol 11:605–623

Ohlemiller KK, Rosen AR, Rellinger EA, Montgomery SC, Gagnon PM (2011) Different cellular and genetic basis of noise-related endocochlear potential reduction in CBA/J and BALB/cJ mice. J Assoc Res Otolaryngol 12:45–58

Okamoto Y, Hoya N, Kamiya K, Fujii M, Ogawa K, Matsunaga T (2005) Permanent threshold shift caused by acute cochlear mitochondrial dysfunction is primarily mediated by degeneration of the lateral wall of the cochlea. Audiol Neuro Otol 10:220–233

Oyamada M, Takebe K, Oyamada Y (2013) Regulation of connexin expression by transcription factors and epigenetic mechanisms. Biochim Biophys Acta Biomembr 1828:118–133

Pauley S, Lai E, Fritzsch B (2006) Foxg1 is required for morphogenesis and histogenesis of the mammalian inner ear. Dev Dyn 235:2470–2482

Riccomagno MM, Martinu L, Mulheisen M, Wu DK, Epstein DJ (2002) Specification of the mammalian cochlea is dependent on Sonic hedgehog. Genes Dev 16:2365–2378

Royaux IE, Suzuki K, Mori A, Katoh R, Everett LA, Kohn LD, Green ED (2000) Pendrin, the protein encoded by the Pendred syndrome gene (PDS), is an apical porter of iodide in the thyroid and is regulated by thyroglobulin in FRTL-5 cells. Endocrinology 141:839–845Rudnicki A, Isakov O, Ushakov K, Shivatzki S, Weiss I, Friedman LM, Shomron N, Avraham KB (2014) Next-generation sequencing of small RNAs from inner ear sensory epithelium identifies microRNAs and defines regulatory pathways. BMC Genomics 15:484

Salt AN, Konishi T (1979) Effects of noise on cochlear potentials and endolymph potassium concentrations recorded with ion-selective electrodes. Hear Res 1:343–363

Schmiedt RA (1993) Cochlear potentials in quiet-aged gerbils: does the aging cochlea need a jump start? In: Verillo RT (ed) Sensory research: multimodal perspectives. Lawrence Erlbaum, Hillsdale, pp 91–103

Schuknecht HF, Gacek MR (1993) Cochlear pathology in presbycusis. Ann Otol Rhinol Laryngol 102:1–16

Schuknecht HF, Watanuki K, Takahashi T, Belal AA, Kimura RS, Jones DD (1974) Atrophy of the stria vascularis, a common cause for hearing loss. Laryngoscope 84:1777–1821

Selvakumar D, Drescher MJ, Dowdall JR, Khan KM, Hatfield JS, Ramakrishnan NA, Drescher DG (2012) CNGA3 is expressed in inner ear hair cells and binds to an intracellular C-terminus domain of EMILIN1. Biochem J 443:463–476

Sewell W (1984) The effects of furosemide on the endocochlear potential and auditory nerve fiber tuning curves in cats. Hear Res 14:305–314

Spicer SS, Schulte BA (2005) Pathologic changes of presbycusis begin in secondary processes and spread to primary processes of strial marginal cells. Hear Res 205:225–240

Spiess AC, Lang H, Schulte BA, Spicer SS, Schmiedt RA (2002) Effects of gap junction uncoupling in the gerbil cochlea. Laryngoscope 112:1635–1641

Summers KM, Bokil NJ, Lu FT, Low JT, Baisden JM, Duffy D, Radford DJ (2010) Mutations at KCNQ1 and an unknown locus cause long QT syndrome in a large Australian family: implications for genetic testing. Am J Med Genet A 152:613–621

Takumida M, Takumida S, Anniko M (2014) Localization of sirtuins in the mouse inner ear. Acta Otolaryngol 134:331–338

Tran Ba Huy P, Ferrary E, Roinel N (1989) Electrochemical and clinical observations in 11 cases of Meniere's disease. In: Nadol JB (ed) Meniere's disease. Kugler and Ghedini, Amsterdam, pp 241–246

Ulehlova L (1983) Stria vascularis in acoustic trauma. Arch Otorhinolaryngol 237:133–138

Varma S, Cao Y, Tagne J-B, Lakshminarayanan M, Li J, Friedman TB, Morell RJ, Warburton D, Kotton DN, Ramirez MI (2012) The transcription factors Grainyhead-like 2 and NK2-homeobox 1 form a regulatory loop that coordinates lung epithelial cell morphogenesis and differentiation. J Biol Chem 287:37282–37295

Vassout P (1984) Effects of pure tone on endocochlear potential and potassium ion concentration in the guinea pig cochlea. Acta OtoLaryngol 98:199–203

Wang W, Lufkin T (2005) *Hmx* homeobox gene function in inner ear and nervous system cell-type specification and development. Exp Cell Res 306:373–379

Wang J, Li Q, Dong W, Chen J (1992) Effects of various noise exposures on endocochlear potentials correlated with cochlear gross responses. Hear Res 59:31–38

Wang Y, Hirose K, Liberman MC (2002) Dynamics of noise-induced cellular injury and repair in the mouse cochlea. J Assoc Res Otolaryngol 3:248–268

Wangemann P (2006) Supporting sensory transduction: cochlear fluid homeostasis and the endocochlear potential. J Physiol 576(1):11–21

Watanabe K, Takeda K, Katori Y, Ikeda K, Oshima T, Yasumoto K, Saito H, Takasaka T, Shibahara S (2000) Expression of the Sox10 gene during mouse inner ear development. Mol Brain Res 84:141–145

Willott JF, Turner JG, Carlson S, Ding D, Bross LS, Falls WA (1998) The BALB/c mouse as an animal model for progressive sensorineural hearing loss. Hear Res 115:162–174

Xiao S-M, Kung AWC, Gao Y, Lau KS, Ma A, Zhang ZL, Liu JM, Xia W, He J-W, Zhao L, Nie M, Fu WZ, Zhang MJ, Sun J, Kwan JSH, Tso GHW, Dai ZJ, Cheung CL, Bow CH, Leung AYH, Tan KCB, Sham PC (2012) Post-genome wide association studies and functional analyses identify association of MPP7 gene variants with site-specific bone mineral density. Hum Mol Genet 21:1648–1657

Yang H, Zhao X, Xu Y, Wang L, He A, Lundberg YW (2011) Matrix recruitment and calcium sequestration for spatial specific otoconia development. PLoS One 6, e20498